Available online at www.sciencedirect.com
SCIENCE DIRECT®
Coordination Chemistry Reviews 249 (2005) 1776–1796
COORDINATION CHEMISTRY REVIEWS
www.elsevier.com/locate/ccr

Review

Recent advances in polyoxometalate-containing molecular conductors

Eugenio Coronado *, Carlos Giménez-Saiz, Carlos J. Gómez-García

Institut de Ciència Molecular (ICMol), Universitat de València, Departamento Qumica Inorgnica, Doctor Moliner, 50, E46100 Burjassot Valencia, Spain

Received 15 November 2004; accepted 22 February 2005
Available online 6 April 2005

Contents

Abstract

The recent advances in crystalline conducting molecular materials based on polyoxometalates (POMs) and organic donors of the tetrathiafulvalene (TTF) family or perylene are discussed. We emphasise the wide diversity of POM structural types and the variety of packing architectures for the organic molecules that can be induced by these inorganic anions. Besides structural effects, we show that these hybrids can have interesting electric and/or magnetic properties. Thus, in the last years the common belief that this type of radical salts containing such big and highly charged anions could only exhibit poor conducting properties has been refuted by the production of new materials exhibiting higher and higher conductivities and even metallic behavior down to very low temperatures.

Keywords: Polyoxometalates; Tetrathiafulvalene; Conducting materials; Molecular hybrids

Abbreviations: BEDO-TTF or BEDO, bis(ethylenedioxy)tetrathiafulvalene; BEDS-TTF or BEST, bis(ethylenediseleno)tetrathiafulvalene; BEDT-TSF or BETS, bis(ethylenedithio)tetraselenafulvalene; BEDT-TTF or ET, bis(ethylenedithio)tetrathiafulvalene; BET-TTF or BET, bis(ethylenethio)tetrathiafulvalene; per, perylene; DMCTTF, dimethyltetramethylenetetrathiafulvalene; DMDPhTTF, dimethyldiphenyltetrathiafulvalene; DMF, N,N-dimethylformamide; EDT-TTF, ethylenedithiotetrathiafulvalene; POM, polyoxometalate; TCNQ, tetracyano-*p*-quino-dimethane; THF, tetrahydrofurane; TMTSF, tetramethyltetraselenafulvalene; TMTTF, tetramethyltetrathiafulvalene; TPhTTF, tetraphenyltetrathiafulvalene; TTF, tetrathiafulvalene

* Corresponding author. Tel.: +34 96 3544859; fax: +34 96 3544859.
E-mail address: eugenio.coronado@uv.es (E. Coronado).

0010-8545/$ – see front matter © 2005 Elsevier B.V. All rights reserved.
doi:10.1016/j.ccr.2005.02.017

1. Introduction

The field of molecular materials with electrical properties started in 1965 with the discovery of the first molecular conductor, the salt (*N*-methylphenazenium)(TCNQ) [1] (TCNQ, tetracyano-*p*-quino-dimethane) followed by the discovery in 1973 of the salt (TTF)(TCNQ) [2] (TTF, tetrathiafulvalene), which constitutes the first example of a metallic charge transfer complex containing the organic donor TTF (see Fig. 1a). Since then, the synthesis of radical salts and charge transfer complexes with TTF and its derivatives has given rise to thousands of molecular semiconductors, hundreds of metals and almost a hundred superconductors. The first of these molecular superconductors, the salts $[TMTSF]_2X$ ($X = [PF_6]^-$, $[AsF_6]^-$; TMTSF, tetramethyl-tetraselenafulvalene), were reported in 1979 [3]. In the last two decades the search for these materials has witnessed rapid development. Many new molecules have been designed which, when assembled in the appropriate manner in the solid, have allowed researchers to improve the conducting properties and even to increase the superconducting critical temperatures.

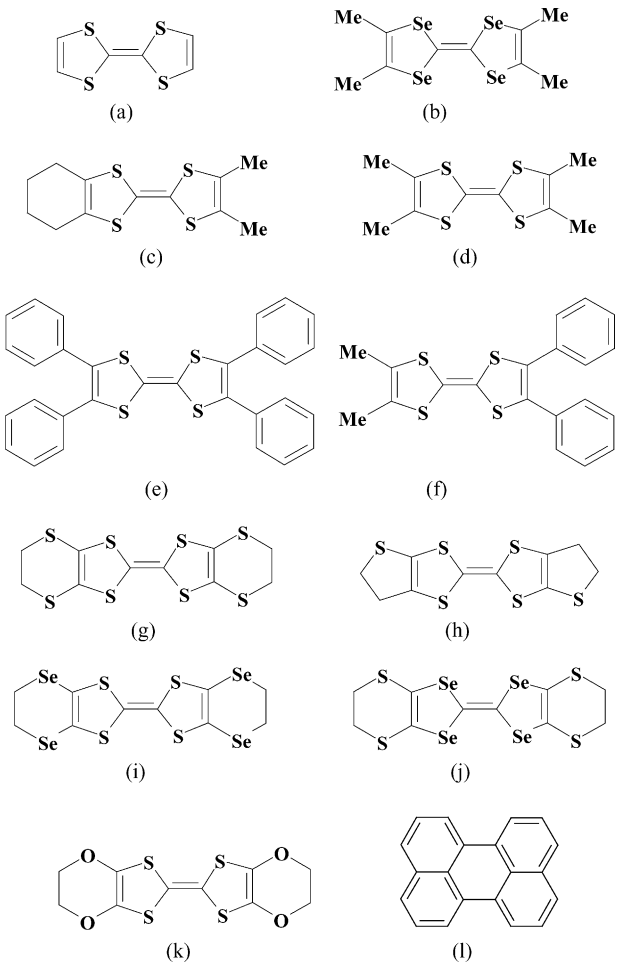

Fig. 1. Organic donors that have been combined with POMs: (a) TTF, (b) TMTSF, (c) DMCTTF, (d) TMTTF, (e) TPhTTF, (f) DMDPhTTF, (g) BEDT-TTF or ET, (h) BET-TTF or BET, (i) BEDS-TTF or BEST, (j) BEDT-TSF or BETS, (k) BEDO-TTF or BEDO, (l) perylene (per).

Recently, a new trend in the field of molecule-based materials started to develop: the design of multifunctional materials that combine properties not normally associated with a single material. Some intriguing applications of this concept would be to couple conductivity with magnetic properties. In fact, this goal was proposed [4] in the mid 1980's but has only recently begun to afford the first successful results. Thus, although there are many examples of molecular materials exhibiting magnetic, electrical or optical properties, only very few of them present two or more of these properties simultaneously. Among them, the most significant examples in the field of magnetic conductors are probably: (i) the synthesis in 1990 of $[ET]_3[CuCl_4]\cdot H_2O$, the first molecular metallic conductor with a paramagnetic center [5] (ii) the synthesis in 1995 of $[ET]_4[(H_3O)Fe(ox)_3]\cdot$solvent [6], (ox = oxalate anion = $C_2O_4^{2-}$) and, in 1996, of λ-$[BETS]_2[FeCl_4]_{0.5}[GaCl_4]_{0.5}$ [7], the first molecular superconductors with paramagnetic centers and (iii) the recent synthesis in 2000 of the layered material $[ET]_3[MnCr(ox)_3]$, the first molecular material that shows coexistence of ferromagnetism and metallic conductivity [8]. A recent review covering the advances in this area has just appeared [9].

As can be seen from the aforementioned examples, the electrical properties are usually provided by organic donors of the TTF family, mainly ET (see Fig. 1), whereas the magnetic properties arise from simple inorganic molecular anions, as in (i) and (ii), or from more complex extended magnetic layers, as in (iii). Nevertheless, these are not the only bricks that can be used to construct multifunctional molecular materials. In between these two limits (molecular anions and extended lattices) one can find the so-called polyoxometalate anions (POMs), i.e., soluble molecular clusters of metal oxides of nanometric size. These anions have shown to be suitable inorganic building blocks to be combined with organic donors for several reasons (see below). As organic molecular components the choice is not limited to TTF type molecules; perylene donors and conducting polymers can also be used in order to introduce electron delocalization in the solid. The organic donors and the POMs used so far to form the POM-containing radical salts are listed in Figs. 1 and 2, respectively.

Since 1988, in which the first POM-containing radical salt of TTF was reported [10a], a large number of conducting materials containing POMs with different topologies, charges, chemical compositions and magnetic moments have been obtained and characterized. Most of these materials exhibit unusual structural and electronic features which are induced by the special characteristics of POMs. These kind of materials were the subject in 1998 of an exhaustive review [11] in which it became clear that, although POMs were very useful and versatile building blocks for the preparation of hybrid molecular materials, the resulting materials exhibited poor electrical conductivities (low conductivities and semiconducting or insulating behavior in most cases). However, in the last few years some important achievements have been accomplished in this area, as for example the discovery of POM-containing radical salts exhibiting high electrical conductivities and even

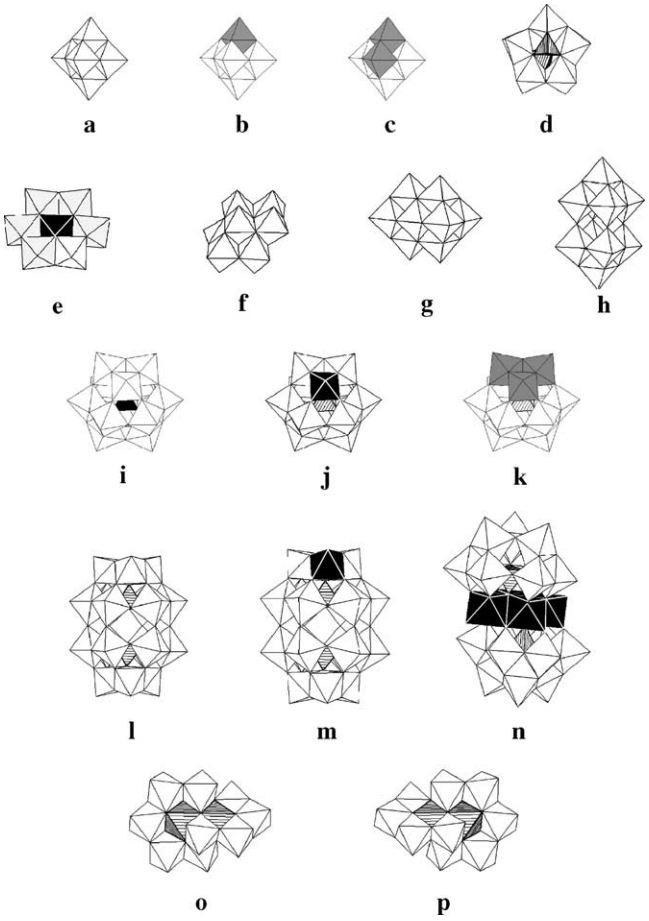

Fig. 2. POM structures used in the synthesis of TTF and perylene-based radical salts: (a) Lindqvist anion $[M_6O_{19}]^{2-}$ (M = Mo or W), (b) monosubstituted Lindqvist anion $[MW_5O_{19}]^{3-}$ (M = V or Nb), (c) disubstituted Lindqvist anion $[HV_2W_4O_{19}]^{3-}$, (d) Strandberg anion, (e) Anderson anion, (f) β-octamolybdate anion β-$[Mo_8O_{26}]^{4-}$, (g) decavanadate anion $[V_{10}O_{28}]^{6-}$, (h) decatungstate anion $[W_{10}O_{32}]^{4-}$, (i) Keggin anion $[X^{n+}M_{12}O_{40}]^{(8-n)-}$ (M = W or Mo; X = B^{III}, Si^{IV}, P^{V}, S^{VI}, H_2^{2+}, Cu^{II}, Co^{II}, Fe^{III}), (j) monosubstituted Keggin anion $[X^{n+}Z^{m+}(H_2O)M_{11}O_{39}]^{(12-n-m)-}$ (X = Si^{IV} or P^{V}; M = W or Mo; Z = Cu^{II}, Co^{II}, Ni^{II}, Mn^{II}, Zn^{II}, Fe^{III}; Cr^{III}), (k) trisubstituted Keggin anion, (l) Dawson–Wells anion, (m) monosubstituted Dawson–Wells anion, (n) $[M_4(H_2O)_2(PW_9O_{34})_2]^{10-}$ (M = Co^{II}, Mn^{II}) (o) and (p) the two enantiomeric forms of the anion $[H_4Co_2Mo_{10}O_{38}]^{6-}$.

metallic behavior. The present contribution covers the developments reported since 1998.

2. Special features of polyoxometalate-containing molecular conductors

POMs present several important features that make them suitable as inorganic building blocks for the construction of the aforementioned functionally active solids [11,12]. In this section we list these characteristics and briefly mention some examples of hybrid salts in which their properties have been greatly influenced by the presence of these cluster anions.

(i) POMs can be made soluble in polar organic solvents and are very stable, maintaining their structure in solution as well as in the solid state. These chemical features provide a means to obtain the solid-state associations of these metal-oxide clusters with the organic donors by using the electrocrystallization technique, which is the usual method of choice for obtaining single crystals of sufficient quality for structural and physical characterizations.
Lindqvist and Keggin-type structures (Fig. 2) are the most stable and chemically versatile POMs. Therefore, they have been extensively used to prepare conducting radical salts of TTF (Table 1), ET (Table 2), BET (Table 3), perylene (Table 4) and other seleniated or oxygenated donors (Table 5). Among the Lindqvist POMs, the ones that have been used are the dianions $[M_6O_{19}]^{2-}$ (M = Mo or W), and the substituted trianions $[M'W_5O_{19}]^{3-}$ (M′ = V or Nb) and $[HV_2W_4O_{19}]^{3-}$. Numerous Keggin POMs have been used including non-substituted anions ($[X^{n+}M_{12}O_{40}]^{(8-n)-}$, where M = W or Mo are the constituent atoms, and X is an heteroatom which can be magnetic or diamagnetic X = B^{III}, Si^{IV}, P^{V}, S^{VI}, H_2^{2+}, Cu^{II}, Co^{II}, Fe^{III}), and monosubstituted anions of general formula $[X^{n+}Z^{m+}(H_2O)M_{11}O_{39}]^{(12-n-m)-}$, where Z is a 3d transition metal ion which replaces one of the external constituent atoms (Z = Cu^{II}, Co^{II}, Ni^{II}, Mn^{II}, Zn^{II}, Fe^{III}; Cr^{III}).

(ii) POMs are bulky anions which, due to the variety of shapes and large sizes they exhibit, can induce new organic packing architectures and, therefore, new band structures and electrical properties. In fact, the crystal structures of these organic–inorganic hybrid materials are the result of the tendency of the planar organic molecules to stack and that of the inorganic metal-oxide clusters to adopt closed-packed lattices.
In general, the POM-containing radical salts of the TTF type, or other related donors containing only inner chalcogen atoms such as TMTTF or TMTSF, have a marked tendency to afford 1D packing architectures as in other TTF-based materials containing simple monoanions. Examples of this kind are provided by the hybrids salts of these donors and Keggin polyanions [10a,13], (salts **1**–**4**) or the salts **6**–**11** which contain Lindqvist type polyanions with stoichiometry 3:1 (salts **6**–**10**) [14,15] or 4:1 (salt **11**) [16]. The 1D organic chains in these salts are formed by dimers (as in the Lindqvist salt **11**), trimers (as in the Lindqvist salts **6**–**10**) or are weakly tetramerized as a consequence of a Peierls-like distortion (Keggin salts **1**–**4**).
However, other radical salts of this type of donors afford unusual organic packing architectures. An example is provided by the phases containing Lindqvist polyanions with a donor:anion stoichiometry of 2:1 (salts **12**–**18**) [14c,14d,17]. These phases do not show chains as in the 3:1 or 4:1 phases but rather isolated dimers of radical cations interspersed with the polyanions. Accordingly,

Table 1
Structure and properties of radical salts containing TTF (or other simple derivatives) and POMs

	Radical salt	Structure	Properties	References
Keggin polyoxometalates				
1	$[TTF]_6[SiMo_{12}O_{40}](NEt_4)$	1D eclipsed stacks of TTFs and isolated neutral TTFs	Semiconductor ($\sigma_{RT} = 10^{-4}$ S cm^{-1})	[13a,13b,13c,13e]
2	$[TTF]_6[PMo_{12}O_{40}](NEt_4)$	Same as **1**	Semiconductor ($\sigma_{RT} = 5 \times 10^{-2}$ S cm^{-1}) Paramagnetic	[13]
3	$[TTF]_6[SiW_{12}O_{40}](NEt_4)$	Same as **1**	Semiconductor ($\sigma_{RT} = 5 \times 10^{-4}$ S cm^{-1})	[13b]
4	$[TTF]_6[PW_{12}O_{40}](NEt_4)$	Same as **1**	Semiconductor ($\sigma_{RT} = 3 \times 10^{-2}$ S cm^{-1}) Paramagnetic	[10]
5	$[TMTSF]_3[PW_{12}O_{40}]$	Chains of donors formed by alternating dimers and monomers	Insulator	[10b]
Lindqvist anions				
6	$[TTF]_3[W_6O_{19}]$	Chains of trimers	Semiconductor ($\sigma_{RT} = 1.4 \times 10^{-3}$ S cm^{-1})	[14a,14b]
7	$[TTF]_3[Mo_6O_{19}]$	Chains of trimers	Semiconductor ($\sigma_{RT} = 0.5 \times 10^{-3}$ S cm^{-1})	[14c,14d]
8	$[TMTSF]_3[W_6O_{19}]\cdot 2DMF$	Chains of trimers	Semiconductor ($\sigma_{RT} = 1.3$ S cm^{-1}, $E_a = 200$ meV)	[14a,14b]
9	$[TMTSF]_3[VW_5O_{19}]\cdot 2DMF$	Chains of trimers	Insulator	[15]
10	$[TMTSF]_3[NbW_5O_{19}]\cdot 2DMF$	Chains of trimers	Insulator	[15]
11	$[TTF]_4[W_6O_{19}]\cdot ½CH_3CN$	Chains of dimers separated by isolated molecules	Insulator	[16]
12	$[TTF]_2[W_6O_{19}]$	Isolated dimers of TTFs	Insulator diamagnetic	[14c,14d]
13	$[TTF]_2[Mo_6O_{19}]$	Isolated dimers of TTFs	Insulator diamagnetic	[14c,14d]
14	$[TMTTF]_2[W_6O_{19}]$	Isolated dimers of TMTTFs	Insulator diamagnetic	[17a]
15	$[TMTTF]_2[Mo_6O_{19}]$	Isolated dimers of TMTTFs	Insulator diamagnetic	[17a]
16	$[TPhTTF]_2[W_6O_{19}]$	Isolated dimers of TPhTTFs	Insulator diamagnetic	[17b]
17	$[DMDPhTTF]_2[Mo_6O_{19}]$	Isolated dimers of DMDPhTTFs	Insulator diamagnetic	[17c]
18	$[DMCTTF]_2[Mo_6O_{19}]$	Isolated dimers of DMCTTFs	Insulator diamagnetic	[17d]
Other polyoxomolybdates				
19	$[TTF]_7[Mo_8O_{26}]$	Irregular chain packing of TTFs with strong interchain S···S interactions	Semiconductor ($\sigma_{RT} \sim 10^{-3}$ S cm^{-1})	[19]
20	$[TTF]_3[S_2Mo_5O_{23}]_2(NMe_4)_6\cdot 2CH_3CN$	Well isolated chains made of TTF trimers	Insulator	[20]
21	$[TTF]_3[Cr(OH)_6Mo_6O_{18}]\cdot 2CH_3CN\cdot 8H_2O$	Structure not solved	Insulator	[15]

these phases are diamagnetic insulators. The fact that the dimers are fairly well isolated renders these compounds suitable as model systems for studying the coupling of electrons with molecular motions in radical salts of TTF [18]. Other novel and original organic packing architectures of TTF have been observed by using the elongated anion β-$[Mo_8O_{26}]^{4-}$ (Fig. 2f) and the planar anion $[S_2Mo_5O_{23}]^{4-}$ (Fig. 2d) which give rise to the radical salts **19** and **20**, respectively. Compound **19** [19] exhibits an irregular chain packing having strong interchain interactions through the sulfur atoms of TTF molecules, giving rise to an increase of the organic dimensionality. In contrast, the structure of compound **20** [20] is made of channels formed by the polyanions and NMe_4^+ cations in which well isolated TTF chains reside. A larger variety of novel organic structural types are observed among the structures of radical salts based on ET (Table 2). This donor (Fig. 1g) contains outer chalcogen atoms which allow for an increase in the dimensionality of the organic sublattice, giving rise to layered structures and quasi two-dimensional (2D) conductors. Examples are the radical salts with Lindqvist POMs with stoichiometries 2:1 (salts **22** and **23**) [17b,21], 5:1 (salts **24** and **25**) [15,22] and 6:1 (salts **26** and **27**) [15,23]. Also with Keggin POMs the structures usually consist of alternating inorganic and organic layers. Thus, radical salts with three different stoichiometries are obtained with ET and Keggin-type polyanions: 3:1 (salt **28**) [12b], 6:1 (salt **29**) [24] and 8:1. The 8:1 stoichiometry is obtained with nonsubstituted (salts **30**–**42**) [25] and monosubstituted α-Keggin anions (salts **43**–**51**) [26]. The 8:1 compounds crystallize in three closely related structure types namely α_1 (salts **30**–**37**), α_2 (salts **38**–**49**) and α_3 (salts **50**–**51**), all consisting of alternating layers of POMs and ET radicals with an α-packing mode. The organic layers are made of two types of stacks: a dimerized chain and an eclipsed, regular one. In the α_3 phase the Keggin units are linked through a bridging oxygen atom

Table 2
Structure and properties of radical salts containing BEDT-TTF (ET) and polyoxometalates (POMs)

	Radical salt	Structure	Properties	References
Linqvist polyoxometalates				
22	$[ET]_2[Mo_6O_{19}]$	Layers formed by orthogonal ET dimers	Insulator	[17b,21]
23	$[ET]_2[W_6O_{19}]$	Layers formed by orthogonal ET dimers	Insulator	[17b,21]
24	$[ET]_5[VW_5O_{19}]\cdot 5H_2O$	ET layers (β-phase)	M-I transition at 250 K due to crystal cracks	[22]
25	$[ET]_5[HV_2W_4O_{19}]\cdot 5H_2O$	Same as **24**	The crystal cracks near RT ($\sigma_{RT} = 6.8 \times 10^{-3}$ S cm^{-1})	[15]
26	$[ET]_6[VW_5O_{19}]\cdot DMF\cdot 2H_2O$	ET layers (α-phase)	Semiconductor ($\sigma_{RT} = 1.1$ S cm^{-1})	[23]
27	$[ET]_6[NbW_5O_{19}]\cdot$solvent	Structure not solved; probably isostructural to **26**	Probably similar to **26**	[15]
Keggin polyoxometalates				
28	$[ET]_3[PW_{12}O_{40}]\cdot n$THF	Not reported	Not reported	[12b]
29	$[ET]_6[PMo_{12}O_{40}]\cdot 4CH_3CN\cdot 6H_2O$	ET layers (variant of the α phase)	Semiconductor ($\sigma_{RT} = 2$ S cm^{-1}, $E_a = 78$ meV) paramagnetic	[24]
30	α_1-$[ET]_8[SiW_{12}O_{40}]$	ET layers (α-phase) formed by alternating eclipsed and dimerized stacks; there are three independent ETs; the POM's layers show a 2D arrangement	Semiconductor ($\sigma_{RT} = 0.15$ S cm^{-1}, $E_a \sim 100$ meV)	[25a,25f,25c,25d,25g]
31	α_1-$[ET]_8[PMo_{12}O_{40}]$	Same as **30**	Semiconductor ($\sigma_{RT} = 0.1$ S cm^{-1}, $E_a \sim 180$ meV)	[25f,25g]
32	α_1-$[ET]_8[SiMo_{12}O_{40}]$	Same as **30**	Semiconductor ($\sigma_{RT} = 1.5 \times 10^{-3}$ S cm^{-1})	[25h]
33	α_1-$[ET]_8[CoW_{12}O_{40}]\cdot 5.5H_2O$	Same as **30**	Semiconductor ($\sigma_{RT} = 0.07$ S cm^{-1}, $E_a = 120$ meV)	[25b,25c,25d]
34	α_1-$[ET]_8[FeW_{12}O_{40}]\cdot 9H_2O$	Same as **30**	Semiconductor	[25c,25d]
35	α_1-$[ET]_8[CuW_{12}O_{40}]$	Same as **30**	Semiconductor	[25c,25d]
36	α_1-$[ET]_8[H_2W_{12}O_{40}]$	Same as **30**	Semiconductor	[25c,25d]
37	α_1-$[ET]_8[SMo_{12}O_{40}]$	Same as **30**	Semiconductor	[33]
38	α_2-$[ET]_8[CoW_{12}O_{40}]\cdot 1/2CH_3CN\cdot 3H_2O$	Similar to the α_1 phases (**30**–**37**), but there are only two independent ETs and the unit cell parameters are different; the POM's layers adopt an intermediate dimensionality between that of the α_1 and α_3 phases (**50**–**51**)	Semiconductor	[25c,25d]
39	α_2-$[ET]_8[BW_{12}O_{40}]\cdot 2H_2O$	Same as **38**	Semiconductor ($\sigma_{RT} = 0.03$ S cm^{-1}, $E_a = 160$ meV)	[25c,25d]
40	α_2-$[ET]_8[CuW_{12}O_{40}]$	Same as **38**	Semiconductor	[25c,25d]
41	α_2-$[ET]_8[FeW_{12}O_{40}]$	Same as **38**	Semiconductor	[25c,25d]
42	α_2-$[ET]_8[H_2W_{12}O_{40}]$	Same as **38**	Semiconductor	[25c,25d]
43	α_2-$[ET]_8[SiFe(H_2O)Mo_{11}O_{39}]$	Same as **38**	Semiconductor	[26c]
44	α_2-$[ET]_8[PZn(H_2O)W_{11}O_{39}]$	Same as **38**	Semiconductor	[26c]
45	α_2-$[ET]_8[PCo(H_2O)W_{11}O_{39}]$	Same as **38**	Semiconductor	[26c]
46	α_2-$[ET]_8[PCu(H_2O)W_{11}O_{39}]$	Same as **38**	Semiconductor ($\sigma_{RT} = 7 \times 10^{-3}$ S cm^{-1}, $E_a \sim 80$ meV)	[26c]
47	α_2-$[ET]_8[SiCu(H_2O)Mo_{11}O_{39}]$	Same as **38**	Semiconductor	[34]
48	α_2-$[ET]_8[SiCr(H_2O)W_{11}O_{39}]$	Same as **38**	Semiconductor	[26b,26c]
49	α_2-$[ET]_8[PNi(H_2O)W_{11}O_{39}]\cdot 2H_2O$	Same as **38**	Semiconductor	[26c]
50	α_3-$[ET]_{8n}[PMn(H_2O)W_{11}O_{39}]_n\cdot 2nH_2O$	Similar to the α_1 phase (**30**–**37**), but the unit cell parameters are different; the Keggin units are linked through a bridging O atom giving rise to a 1D chain	Semiconductor ($\sigma_{RT} \sim 0.1$ S cm^{-1})	[26a,26b,26c]

Table 2 (*Continued*)

	Radical salt	Structure	Properties	References
51	α_3-[ET]$_{8n}$[PMn(H$_2$O)Mo$_{11}$O$_{39}$]$_n$	Same as **50**	Semiconductor	[26c]
52	[ET]$_8$[PMo$_3$NbW$_8$O$_{40}$]	Probably isostructural to the α_1 phase (**30**–**37**)	Semiconductor	[48]
53	α_1-[ET]$_8$[PMo$_3$W$_9$O$_{40}$]	Isostructural to the other α_1 salts (**30**–**37**)	Semiconductor (σ_{RT} ~8×10^{-3} S cm^{-1}, E_a ~85 meV)	[49]
54	α_1-[ET]$_8$[PNbW$_{11}$O$_{39}$S]	Isostructural to the other α_1 salts (**30**–**37**)	Semiconductor (σ_{RT} ~0.01 S cm^{-1})	[34]
Dawson polyoxometalates				
55	[ET]$_{11}$[P$_2$W$_{18}$O$_{62}$]·H$_2$O	ET layers (β-phase) formed by zigzag chains	M-I transition at 220 K	[27a,27b]
56	[ET]$_{11}$[P$_2$ReW$_{17}$O$_{62}$]·3H$_2$O	Isostructural to **55**	M-I transition at 250 K	[27c]
Other isopolyoxometalates				
57	[ET]$_4$K$_2$[Mo$_8$O$_{26}$]·DMF	ET layers (pseudo-κ)	Semiconductor (σ_{RT} ~2×10^{-4} S cm^{-1}; E_a = 230 meV)	[45]
58	[ET]$_6$[Mo$_8$O$_{26}$]·3DMF	ET layers (β phase)	M-I transition at 60 K	[46]
59	[ET]$_4$[W$_{10}$O$_{32}$]	Chains of dimers of ETs surrounded by chains of POMs in a chessboard-like arrangement	Insulator	[45]
60	[ET]$_5$[H$_3$V$_{10}$O$_{28}$]·4H$_2$O	ET layers (β phase) made up of ladder chains	M-I transition at 135 K	[42]
Other heteropolyoxometalates				
61	[ET]$_6$H$_4$[Co$_4$(H$_2$O)$_2$(PW$_9$O$_{34}$)$_2$]	Structure not solved	Insulator; Contains a ferromagnetic Co$_4$ cluster in the POM	[28]
62	[ET]$_6$H$_4$[Mn$_4$(H$_2$O)$_2$(PW$_9$O$_{34}$)$_2$]	Structure not solved	Insulator; Contains an antiferromagnetic Mn$_4$ cluster in the POM	[28]
63	[ET]$_4$[Cr(OH)$_6$Mo$_6$O$_{18}$]·2H$_2$O	ET layers (β phase); the POMs form regular face-to-face stacks	Insulator	[52]
64	[ET]$_9$[H$_4$Co$_2$Mo$_{10}$O$_{38}$]·4H$_2$O	ET layers made up of eclipsed stacks; the POM's layers comprise stacks made up of only one enantiomer	Semiconductor (σ_{RT} = 9 S cm^{-1}; E_a = 40 meV)	[55]

Table 3
Structure and properties of radical salts containing perylene (per) and polyoxometalates (POMs)

	Radical salt	Structure	Properties	References
Linqvist polyoxometalates				
65	(per)$_5$[Mo$_6$O$_{19}$]	Organic layers alternated with mixed layers formed by POMs and isolated per molecules	Diamagnetic. semiconductor (σ_{RT} ~0.2 S cm^{-1}; E_a = 194 meV) S (300 K) = 610 μS K^{-1}	[31]
66	(per)$_5$[W$_6$O$_{19}$]	Similar to **65**	Diamagnetic. semiconductor (σ_{RT} ~0.8 S cm^{-1}; E_a = 212 meV) S (300 K) = 230 μS K^{-1}	[31]
67	(per)$_5$[VW$_5$O$_{19}$]	Similar to **65**	Paramagnetic semiconductor (σ_{RT} ~3 S cm^{-1}; E_a = 129 meV) S (300 K) = −350 μS K^{-1}	[31]
Keggin polyoxometalates				
68	(per)$_6$[PMo$_{12}$O$_{40}$]·CH$_2$Cl$_2$	The POM's form channels occupied by two different stacks and isolated per molecules	Two semiconducting regimes separated by a structural transition at ~150 K: 1. (σ_{RT} = 69 S cm^{-1}; E_a = 28.5 meV); 2. E_a = 40.8 meV	[32]
69	(per)$_6$[PMo$_{12}$O$_{40}$]·CH$_3$CN	Isostructural to **68**	Semiconductor (σ_{RT} = 3.6 S cm^{-1}; E_a = 32 meV) S (300 K) = 14.9 μS K^{-1}	[32]
70	(per)$_9$[SiW$_{12}$O$_{40}$]$_2$(NBu$_4$)$_4$	The POM's form channels occupied by per stacks, isolated per molecules and NBu$_4^+$ cations	Semiconductor (σ_{RT} = 0.85 S cm^{-1}; E_a = 101 meV) S (300 K) = −676 μS K^{-1}	[32]

Table 4
Structure and properties of radical salts containing BET-TTF (BET) and polyoxometalates

	Radical salt	Structure	Properties	References
Linqvist polyoxometalates				
71	$[BET]_2[W_6O_{19}]$	Dimers of BETs surrounded by POMs in a chessboard-like arrangement	Insulator	[30]
72	$[BET]_2[Mo_6O_{19}]$	Isostructural to **71**	Insulator	[30]
Keggin polyoxometalates				
73	$[BET]_4[SiW_{12}O_{40}]\cdot CH_3CN\cdot 2H_2O$	The POMs form a 2D hexagonal packing, leaving cavities occupied by BET dimers partially disordered	Insulator	[30]

Table 5
Structure and properties of radical salts containing seleniated or oxygenated donors and polyoxometalates (POMs)

	Radical salt	Structure	Properties	References
74	$[BEST]_3H[PMo_{12}O_{40}]\cdot CH_3CN\cdot CH_2Cl_2$	Interpenetrated layers of POMs and BESTs	Insulator paramagnetic	[29]
75	α_1-$[BETS]_8[SMo_{12}O_{40}]$	Isostructural to the other α_1 salts (**30**–**37**)	Several regimes	[62]
76	$[BEDO]_6K_2[BW_{12}O_{40}]\cdot 11H_2O$	Layers of BEDOs (β phase) and layers of POMs and intercalated K^+ cations	Metallic down to 2 K	[63]

which gives rise to an unprecedented chain of Keggin anions. This result shows that also the organic part is able to induce novel POM structures.

POMs having higher nuclearities and different shapes have also been combined with ET. For example, with the Dawson–Wells POMs $[P_2W_{18}O_{62}]^{6-}$ and $[P_2ReOW_{17}O_{61}]^{6-}$ (Fig. 2l and m) two isostructural compounds have been obtained (salts **55** and **56**) [27]. Their structures consist of alternating layers of polyanions and ET molecules which exhibit the β phase type of packing and are formed by parallel chains of ETs stacked in an exotic zigzag manner. Interestingly, six crystallographically different ET molecules can be distinguished.

Even bigger POMs, such as the anions $[M_4(H_2O)_2(PW_9O_{34})_2]^{10-}$ ($M = Co^{II}$ or Mn^{II}) (Fig. 2n) have been combined with ET to yield radical salts with a 6:1 stoichiometry (salts **61** and **62**) [28] although their crystal structure could not be solved.

Other organic donors have also been combined with POMs. For example, BEST (Fig. 1i) has been combined with the Keggin anion $[PMo_{12}O_{40}]^{3-}$ to afford the radical salt **74**, which exhibits an unusual structure with a quasi 3D organic packing [29]. The structure and properties of this compound are discussed in more detail in the next section. BET (Fig. 1h) is another interesting donor that has been combined with POMs, although it has usually given rise to poor quality crystals. For this reason only three radical salts of this donor have been studied with two Lindqvist anions (the isostructural salts **71** and **72**) and with the Keggin anion $[SiW_{12}O_{40}]^{4-}$ (salt **73**) [30]. By using the Lindqvist polyanions, radical salts with a 2:1 stoichiometry are obtained. The structure consists of face to face $(BET^{\bullet+})_2$ dimers with short contacts between the central C and S atoms, surrounded by polyanions such as to form an unusual 3D packing of cations and anions reminiscent of NaCl. In this structure, short intermolecular contacts between the cation pairs are present along the *a* and *b* directions of the triclinic cell. The structure of the salt **73**, containing a Keggin anion, could not be completely solved as some BETs are disordered within hexagonal channels created by the anions, which form a 2D hexagonal packing.

(iii) POMs offer the possibility of varying the anionic charge while maintaining their structure, enabling the control of the electronic band filling in the resulting radical salt and, therefore, the physical properties.

This feature has been illustrated in the TMTSF: Lindqvist system (salts **8**–**10**) [14,15]. By changing the dianion $[W_6O_{19}]^{2-}$ by the trianions $[VW_5O_{19}]^{3-}$ or $[NbW_5O_{19}]^{3-}$, the organic portion reverts from a mixed-valence state to a completely ionized state. As a consequence, salt **8** is a semiconductor, while salts **9** and **10** are insulators. Other relevant example of this kind is provided by the radical salts of the perylene donor (Fig. 1l) with Lindqvist anions having charges 2− and 3− (salts **65**–**67**) [31]. In this case, isostructural radical salts are obtained which, depending on the charge of the polyanion, show clear differences in the conducting properties and in the mechanism of the conductivity. These salts are discussed in detail in Section 4.1.

(iv) POMs are electron acceptors which, in some cases, can be reduced by one or more electrons to give rise to mixed valence clusters. This enables the formation of hybrid materials in which delocalized electrons coexist in both the organic network and the inorganic clusters.

Examples of this kind are provided by all the radical salts containing the phosphomolybdate anion $[PMo_{12}O_{40}]^{3-}$

which is always reduced by one electron and therefore presents a charge of −4 (with the exception of the perylene salts **68** and **69** where the anion is not reduced) [32]. Salts containing the anions $[SMo_{12}O_{40}]^{2-}$ (**37** and **75**) [33] and $[PMo_3W_9O_{40}]^{3-}$ (**53**) [34] are also formed by reduced anions. In all these salts the presence of delocalized electrons hopping over the metal centers of the inorganic polyanion is demonstrated by EPR spectroscopy.

(v) The large charges and volumes of POMs, which have been considered as an advantage in the previous paragraphs, usually induce irregular stacks and charge localization in the organic sublattice which ultimately leads to poor conducting properties.
A quick look at Tables 1–4 will be enough to check that most of the POM-containing radical salts are insulators or semiconductors. However, few exceptions are known that show metallic behavior at high temperatures and, in one case, down to very low temperatures. The first example that showed a metallic-like behavior was observed in radical salts of ET with the mixed-metal Lindqvist anions $[VW_5O_{19}]^{3-}$ and $[HV_2W_4O_{19}]^{3-}$ with stoichiometry 5:1 (**24** and **25**) [15,22]. At high temperatures increases in the conductivities upon cooling (from $14\,S\,cm^{-1}$ at room temperature to a maximum value of $\sim 30\,S\,cm^{-1}$ at 250 K) were observed in salt **24**. However, below this temperature a metal–insulator transition occurred that was attributed to cracks on the single crystals resulting from a loss of water molecules. More recently other radical salts containing Dawson–Wells POMs (**55** and **56**) [27] have shown to be metallic at temperatures higher than 230 K. At lower temperatures the salts become semiconductors with a very low activation energy value.

(vi) POMs can act as ligands that incorporate one or more paramagnetic transition metals ions at specific sites of the polyoxoanion structure. The introduction of magnetic character into the polyanion can produce novel materials in which delocalized electrons coexist with localized magnetic moments, thus affording the opportunity to obtain molecular systems combining magnetic and conducting properties.
The first radical salts containing paramagnetic POMs were obtained using Keggin polyanions and ET (the α_1, α_2 and α_3 phases mentioned before, see Table 2). In these salts no magnetic effects arising from the d–π interaction between these localized d electrons and the itinerant π electrons were detected down to 2 K. A possible reason for the lack of interactions could be the semiconducting nature of these radical salts. The paramagnetic Dawson–Wells polyanion $[P_2ReOW_{17}O_{61}]^{6-}$ was also combined with ET (salt **56**) [27c]. EPR and magnetic susceptibility measurements confirmed the coexistence of a conducting network with a paramagnetic Re(VI) ($S = 1/2$) center in the polyanion but no significant interactions between both sublattices have been detected, despite the large electron delocalization found in the organic layers. Finally $[M_4(H_2O)_2(PW_9O_{34})_2]^{10-}$ anions ($M = Co^{II}$ and Mn^{II}) encapsulating tetranuclear magnetic clusters between fragments of POMs were combined with ET (salts **61** and **62)** [28]. Again, no interactions between the two spin sublattices were found as these salts are insulators.

3. Molecular conductors based on ET and new polyoxometalates

Two possible strategies have been explored to obtain new POM-containing radical salts exhibiting larger conductivities and/or a metallic-like behavior: (i) the use of POMs different from those combined so far with ET. (ii) The use of other donors. The two types of novel donors that have been used are perylene and the selenium or oxygen derivatives of ET. These donors have shown to provide conducting materials with very high conductivities or even superconductivity when combined with simple anions [3c,35]. In this section we will focus on the results obtained in relation with point (i), while the results obtained in relation with point (ii) will be presented in the next section.

3.1. The polyoxovanadate $[H_3V_{10}O_{28}]^{3-}$

All the previous radical salts were based on polyoxomolybdates and polyoxotungstates. However, vanadium-containing polyoxoanions are interesting as components of new radical salts because they present a wide range of interesting properties associated with their distinctive topologies and electronic structures [36]. These anions can show compact structures like $[V_{10}O_{28}]^{6-}$ [37], (Fig. 2g) open complexes with ribbon, basket, or shell shapes [38], or even close host structures that can uptake neutral or ionic guests [39]. Many giant clusters are also known, for example, the $\{V_{19}\}$ cluster family [40]. Another feature of polyoxovanadates is their remarkable redox processes that make them interesting in several fields, such as magnetochemistry [41].

Recently, we have reported the first polyoxovanadate-containing radical salt [42]. This hybrid compound (salt **60**) is formed by ET and $[H_3V_{10}O_{28}]^{3-}$ and has a donor:anion stoichiometry of 5:1. Its structure is formed by alternating layers of polyoxovanadate anions and cation layers of ET molecules (Fig. 3a). The organic layers adopt a packing motif typical of the so-called β″-phases [43] (Fig. 3b). It is composed of stepwise parallel chains of ETs formed by the repetition of groups of five eclipsed ETs following the sequence . . ., CBABC, ... The chains are displaced to one another with interchain distances being shorter that the intrachain ones. The shortest S · · · S interchain contacts range from 3.32 to 3.55 Å, whereas the intrachain ones range from 3.75 to 3.84 Å. The interchain distances are much shorter that the sum of the van der Waals radii (3.6 Å), showing that the system is really 2D and that

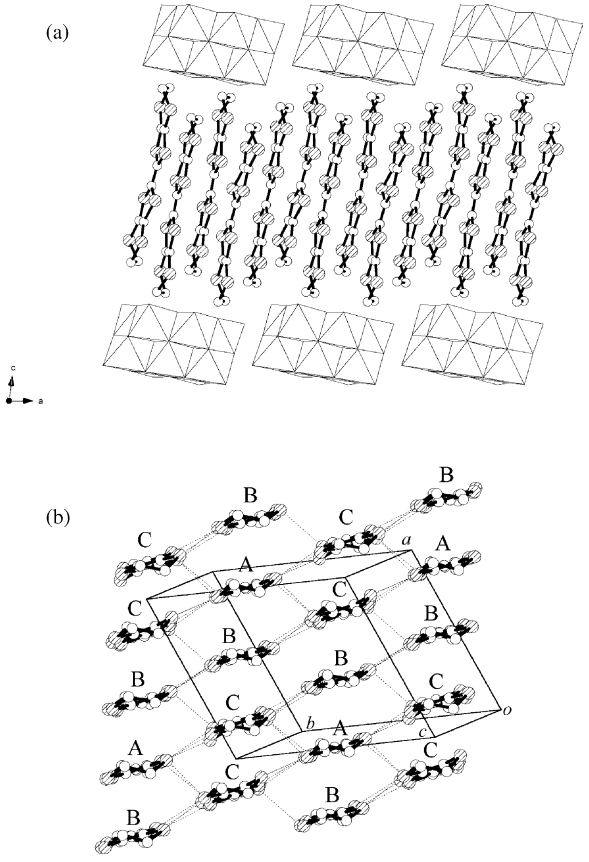

Fig. 3. (a) View along the *b* axis of the alternating organic and inorganic layers of compound **60**. (b) View of the organic layer of compound **60** along the long molecular axis of the ET molecules. The carbon atoms are depicted as white spheres and the sulphur atoms as hatched spheres.

the overlap of the organic radicals is important. Both characteristics are key features for the electrical properties of this material.

The 5:1 stoichiometry suggests a mixed valence state in the organic part, with three positive charges distributed over the five ETs. The degree of ionicity of each ET could be roughly estimated from the bond distances of the fulvalene ring [44], suggesting that A-type molecules are completely ionized, while C and B molecules have a charge close to +0.5, in agreement with the trianionic charge of the polyoxovanadate. The presence of partially oxidized ET molecules in an extended bidimensional network is expected to favor the electrical conductivity. In fact the electrical conductivity at room temperature is very high, 235 S cm^{-1}, and increases up to 350 S cm^{-1} at 135 K (Fig. 4); at lower temperatures a decrease upon further cooling is observed indicating the appearance of a semiconducting regime. The metallic regime at high temperatures was confirmed by thermopower measurements as well as the semiconducting transition at lower temperatures which is associated with the opening of an energy gap around 50 K, preceded by a fluctuating regime with a gradual onset upon cooling below ~140 K.

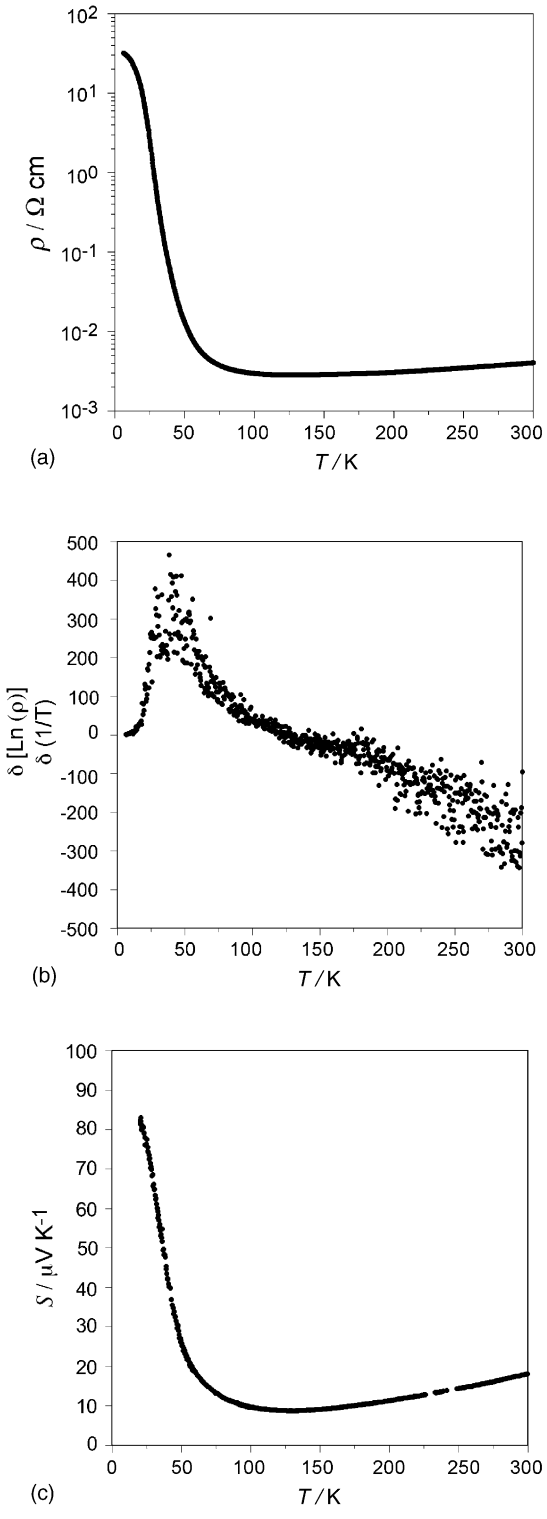

Fig. 4. Electrical transport properties of compound **60**: (a) temperature dependence of the electrical resistivity, ρ, (b) temperature dependence of the derivative $\mathrm{d}\ln\rho/\mathrm{d}(1/T)$, (c) temperature dependence of the Seebeck coefficient.

3.2. The isopolyoxomolybdate β-$[Mo_8O_{24}]^{4-}$

The isopolyoxomolybdate β-$[Mo_8O_{24}]^{4-}$ (Fig. 2f) was first combined with TTF to give rise to salt **19** with a donor:anion stoichiometry 7:1 [19]. In this salt an unprecedented 2D packing of the TTFs was observed having strong intra and interchain interactions, although the displacement of two adjacent organic molecules limited the electronic delocalization, therefore accounting for the semiconducting behavior of this salt. This POM has recently been combined with ET with the aim of improving the contacts between the organic molecules and so the electrical conductivity. Two different phases have been obtained having donor:anion stoichiometries of 4:1 (salt **57**) and 6:1 (salt **58**). Both salts were obtained following similar electrocrystallization procedures but starting from salts $TBA_3K[Mo_8O_{26}]\cdot 2H_2O$ and $TBA_4[Mo_8O_{26}]$, respectively. This accounts for the presence of K^+ ions in **57**.

Compound **57** [45] is formed by alternated layers of ETs and POMs (Fig. 5a). The K^+ cations and solvent molecules are intercalated in between the anions. The organic layers are made of two crystallographically different molecules (A and B) which are arranged forming centrosymmetric dimers (AA) surrounded by six molecules of type B (Fig. 5b). This 2:1 pseudo-κ type of packing resembles that observed in a salt of ET with the $[Cr(ox)_3]^{3-}$ anion [6]. Several S···S intradimer and dimer–monomer contacts are shorter than the sum of the van der Waals radii (ranging between 3.41 and 3.58 Å). The analysis of the bond distances indicates that the two ETs of the dimer (A-type) are completely charged whereas the B-type molecules are neutral. This charge distribution precludes any electron delocalization in the organic layer and, accordingly, compound **57** is a semiconductor with a low room temperature conductivity ($\sim 2\times10^{-4}$ S cm^{-1}) and a high activation energy (230 meV).

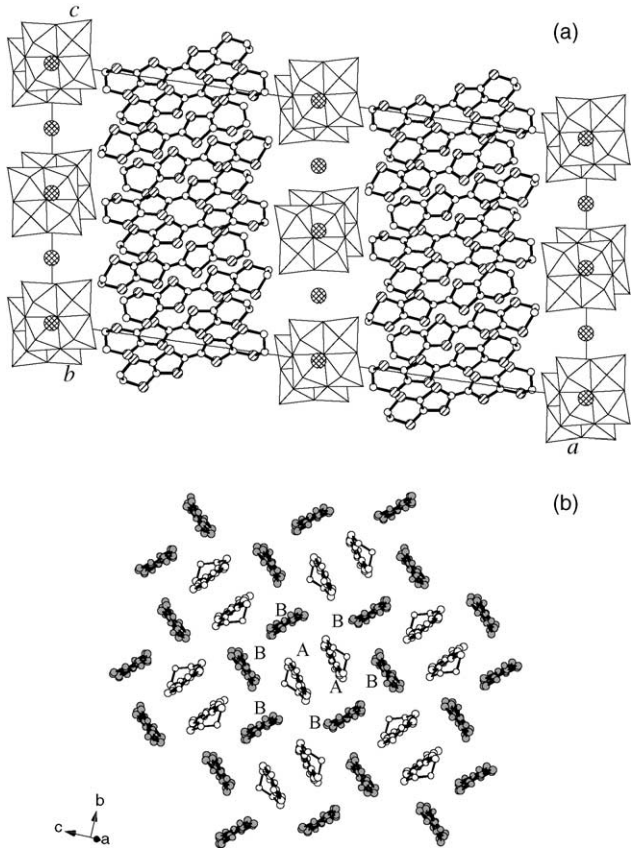

Fig. 5. (a) View along the *b* axis of the structure of the radical salt **57** showing the alternating organic and inorganic layers. The carbon atoms are depicted as white spheres, the sulphur atoms as hatched spheres and the potassium ions as crossed spheres. (b) View of the organic layer of compound **57** along the long molecular axis of the ET molecules. The crystallographically independent ET molecules of type A and B are depicted in white and grey color, respectively.

The synthesis, structure and physical properties of compound **58** have recently been reported by A. Łapiński et al. [46] Its crystal structure is also made of alternating layers of ET molecules and layers of β-$[Mo_8O_{26}]^{4-}$ polyanions and solvent molecules parallel to the *ab* plane (Fig. 6a). The organic layers are made up of three crystallographically different ET molecules, labelled A, B and C, which form stacks following the sequence ..., ABC, ... in one chain, and the reverse sequence in the adjacent stacks (inset in Fig. 6b). There are no intrastack S···S contacts shorter than the sum of the van der Waals radii, although there are many short interstack side-by-side S···S contacts. The existence of partially oxidized ET molecules was confirmed by UV and Raman spectroscopy. The salt exhibits metallic properties at high temperatures (Fig. 6b). The conductivity increases when the temperature is lowered from a value of 3 S cm^{-1} at room temperature to a value of about 12 S cm^{-1} at 60 K. Below this temperature the conductivity shows a sharp decrease reaching a value 5 orders of magnitude lower at about 4 K. An electrical conductivity anomaly was observed at about 180 K and was confirmed by IR measurements. Above that temperature, electron–phonon scattering is the dominant mechanism of the conductivity. Below 180 K the electron–electron interactions become more important. At very low temperatures, the hopping model of the electrical transport becomes the dominant mechanism.

3.3. The isopolyoxotungstate $[W_{10}O_{32}]^{4-}$

The polyanion $[W_{10}O_{32}]^{4-}$ can be considered as formed by the union of two monovacant Lindqvist anions (Fig. 2h). When this anion is combined with ET the salt **59** is obtained [45]. The crystal structure can be described as formed by chains of ET dimers which are surrounded by four parallel chains of POMs and four chains of ET dimers in a chessboard-like arrangement (Fig. 7).

Each dimer is formed by two crystallographically different ET molecules both having a charge of +1. Inside each dimer there are two short S···S contacts (3.52 and 3.55 Å) but there are no short interdimer contacts (>3.64 Å). The integer charge of ET and the absence of delocalization pathways account for the insulating behavior of this compound.

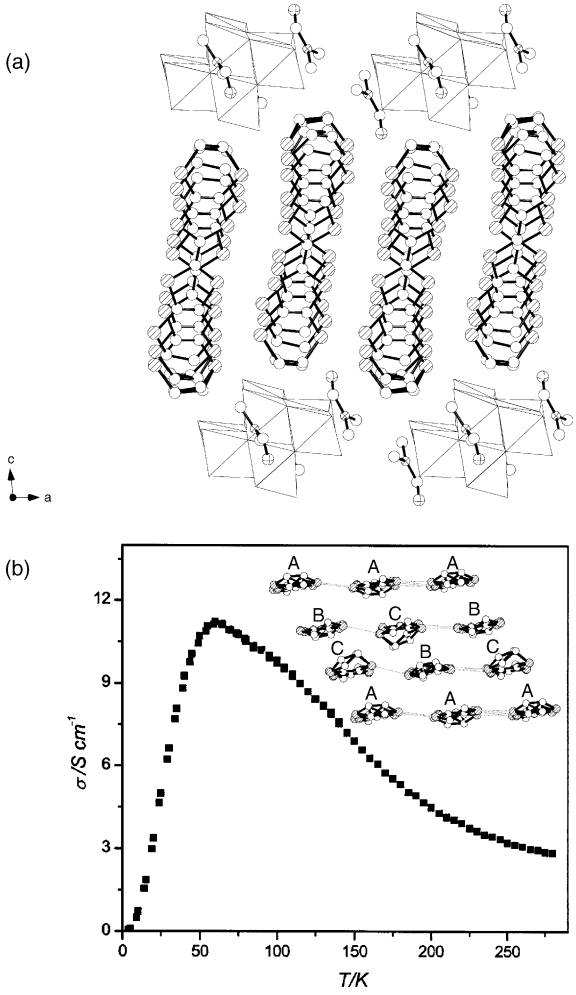

Fig. 6. (a) View along the *b* axis of the structure of compound **58**. (b) Temperature dependence of the dc electrical conductivity of compound **58**. Inset: view of the organic layer of compound **58** along the long molecular axis of the ET molecules. The carbon atoms are depicted as white spheres and the sulphur atoms as hatched spheres. Dotted lines represent S · · · S intermolecular contacts shorter than the sum of the van der Waals radii (3.60 Å).

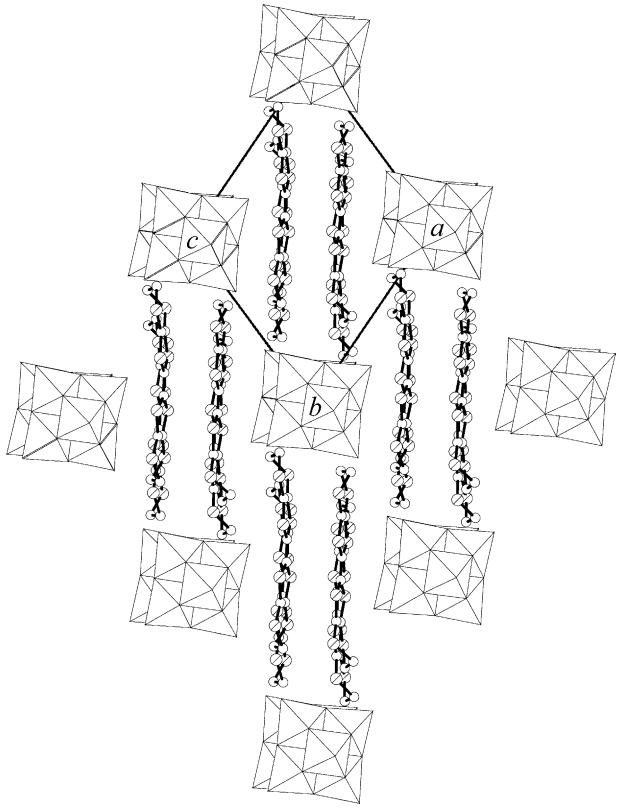

Fig. 7. Projection in the *ac* plane of the structure of compound **59** showing the chessboard arrangement of the chains of ET dimers and POMs. The carbon atoms are depicted as white spheres and the sulphur atoms as hatched spheres.

3.4. Other, less common, Keggin polyoxometalates.

As has been previously mentioned, the nonsubstituted Keggin POMs with general formula $[XM_{12}O_{40}]^{n-}$ can be modified by substitution of one of the constituent metals M, by a first row transition metal Z, giving rise to monosubstituted Keggin polyanions formulated as $[XM_{11}Z(H_2O)O_{39}]^{m-}$. These two kinds of Keggin anions were combined with ET to produce a large family of radical salts having a stoichiometry 8:1. Other chemical modifications are possible within the Keggin structure. For example it is possible to obtain mixed Keggin POMs formed by different constituent atoms, such as Mo, W, V or Nb. This modification produces anions in which the reduction potential depends on the ratio of the constituent atoms in the structure [47]. In general POMs with higher content of Mo are better electron acceptors and so, they can be reduced more easily. The influence of the reduction potential of the Keggin POMs in the formation of radical salts with ET is exemplified by comparing the anions $[PW_{12}O_{40}]^{3-}$ and $[PMo_{12}O_{40}]^{3-}$. While the tungsten derivative only forms one radical salt (**28**) with this donor, the molybdenum derivative (which can be more easily reduced) forms two salts (**29** and **31**). Actually, the reduction of this polyanion has been observed in all the reported radical salts with TTF-type donors (salts **2**, **29**, **31** and **74**).

Up to now $[PMo_3NbW_8O_{40}]^{4-}$ and $[PW_9Mo_3O_{40}]^{3-}$ are the only mixed Keggin POMs that have been combined with ET (salts **52** and **53**). Compound **52** was obtained by Bellito et al. [48] Although its unit cell parameters were not reported, it probably belongs to the α_1 family (see Table 2). In this salt the POM is diamagnetic, as evidenced by the lack of Mo^V signals in the ESR spectrum down to 85 K. The authors also pointed out the possibility that this salt could be a Spin–Peierls system, according to the observed sharp fall in susceptibility at about 7 K. The compound is a semiconductor with a room temperature conductivity of 0.037 S cm^{-1} and an activation energy of 160 meV. Compound **53** crystallizes in the α_1 phase [49] as many of the ET radical salts containing nonsubstituted Keggin polyanions (see Table 2). In this compound the triad of Mo atoms of the $[PW_9Mo_3O_{40}]^{3-}$ anion appears as crystallographically disordered over the 12 possible positions of the Keggin structure. This can be explained by a rotational disorder of the Keggin anions around

the C_2 axis, which makes it appear as a centrosymmetric unit. This kind of disorder has been found in many reported crystal structures of Keggin POMs [50]. ESR measurements on polycrystalline samples indicate that the polyanion is reduced by one electron and that therefore its charge should be −4. The extra electron is delocalized over the three adjacent Mo atoms and therefore its ESR spectrum is different from the spectrum of the isostructural ET salt containing the polyanion $[PMo_{12}O_{40}]^{4-}$, in which the extra electron is fully delocalized over 12 Mo atoms (salt **31**). The conductivity properties of this salt are similar to those of the other members of the α_1 phase. Therefore, salt **53** is a semiconductor with a room temperature conductivity of $\sim 8 \times 10^{-3}$ S cm^{-1} and an activation energy of 85 meV.

Other chemical modifications are possible in the Keggin structure, as for example the substitution of some terminal O atoms by S atoms. In this way polyoxothiometalates can be obtained. The combination of polyoxothiometalates with TTF-type donors is interesting because S···S interactions between the anion and the radical donor can be established (in addition to the S···S interactions between the donors) and this could influence the electronic dimensionality [51]. With this aim the Keggin polyoxothioanion $[PW_{11}NbSO_{39}]^{4-}$, in which the S atoms is bonded to the Nb atom in a terminal position, has been combined with ET (salt **54**) [34]. This compound also crystallizes in the α_1 phase and the crystal structure reveals that the S atom of the POM (and therefore the Nb atom to which it is bonded) is disordered over four positions of the Keggin anion. These positions are lying in the crystallographic *ac* plane, far from the S atoms of the organic donors (Fig. 8). Then, in this case, no S···S interactions are established between the anions and the donors. As the other members of the α_1 family, compound **54** is a semiconductor with a room temperature conductivity of ∼0.01 S cm^{-1}. Other polyoxothiomolybdates with more S atoms in their surface should be combined with TTF-type donors to explore this possibility.

3.5. Planar polyoxometalates

Planar POMs are not very common, Anderson–Evans (Fig. 2e) and Strandberg (Fig. 2d) polyanions being almost the only examples. The combination of planar POMs with TTF-type donors is interesting because due to their planarity they can also form stacks and induce novel packing architectures in the organic sublattice. A radical salt containing the diamagnetic Anderson–Evans polyoxoanion $[TeW_6O_{24}]^{6-}$ and the donor EDT-TTF was reported by Boubekeur et al. [65] in 1998. In the compound, formulated as $[EDT\text{-}TTF]_8\{[Ca(H_2O)_4]_2[TeW_6O_{24}]\cdot 7H_2O\}_2$, the inorganic layers consists of a two-dimensional coordination polymer formed by polyoxometalates and Ca^{2+} cations. The organic sublattice adopts a novel tiling mode of the Kappa slab containing eight crystallographically independent donors (labelled from A to H) organized in two trimeric units and an orthogonal dimer having a net charge distribution of $[(EDT\text{-}TTF^0)_{A,B}(EDT\text{-}TTF)_{C,D,E}{}^{2+}(EDT\text{-}TTF)_{F,G,H}{}^{2+}]$, which accounts for the diamagnetic and insulating nature of the compound. Other radical salts containing the unsymmetrical donor EDT-TTF and Keggin polyoxometalates exhibiting different conductivity properties (from insulating to metallic) have been obtained by the same group by standard and confined electrocrystallization methods [66].

Another radical salt containing the paramagnetic Anderson–Evans polyoxoanion $[Cr(OH)_6Mo_6O_{18}]^{3-}$ and ET was first prepared in 1992 [15] and the crystal structure has recently been reported by Ouahab et al. [52] (salt **63**). Its crystal structure consists of alternating organic and inorganic layers (Fig. 9a). The planar anions are connected

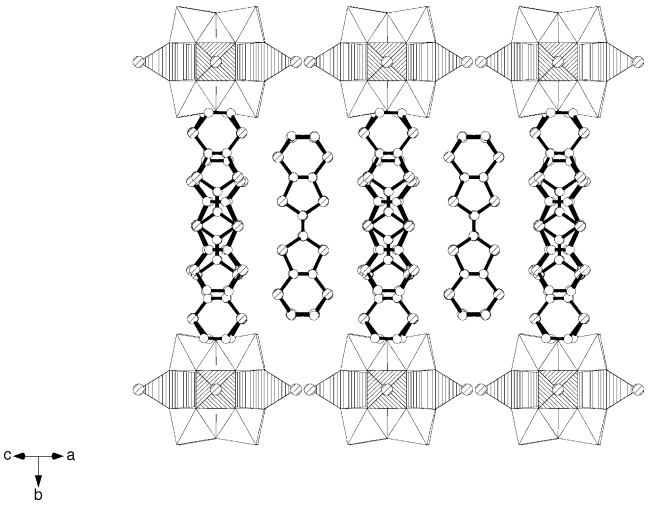

Fig. 8. View of the alternating layers of the structure of compound **54**. The carbon atoms are depicted as white spheres and the sulphur atoms as hatched spheres. The hatched polyhedra indicate the position of the disordered Nb atoms.

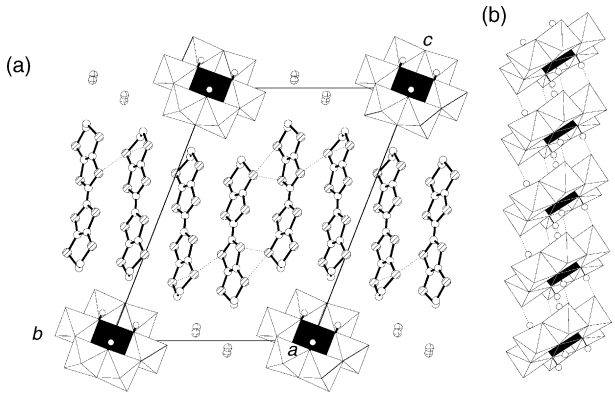

Fig. 9. (a) View of the structure of compound **63** along the *b* axis. The carbon atoms are depicted as white spheres, the sulphur atoms as hatched spheres and the oxygen atoms of water molecules as crossed spheres. Dotted lines represent S···S intermolecular contacts shorter than the sum of the van der Waals radii (3.60 Å). (b) View of the POMs chains of compound **63** along the *a* axis. Dotted lines represent hydrogen bonding between the H atoms of the OH groups bonded to the central Cr atom (inside the black octahedra) of one POM and the terminal oxygen atoms of the next POM.

through short hydrogen bonds and present an unusual face-to-face stacking mode giving rise to infinite regular chains of polyanions parallel to the *a* direction (Fig. 9b). The organic layers exhibit the typical β-type mode of packing and contain dimerized chains parallel to the *b* direction, i.e. perpendicular to the POM chains. There are two crystallographically independent molecules (A and B) which form chains following the sequence . . ., AABB, ... The two types of alternating dimers bear different charges (1.2(1) and 1.7(1) for the AA and BB dimers, respectively) accounting for the insulating nature of this radical salt. Magnetic measurements indicate the absence of significant exchange coupling between the $ET^{\bullet+}$ radicals and the Cr(III) spins located at the Anderson polyanions [15].

Another interesting planar POM is the diamagnetic hexaanion $[H_4Co_2Mo_{10}O_{38}]^{6-}$ which has the additional feature that can exist in two enantiomeric forms (Fig. 2o and p). Chirality is an aspect of POMs that has not been exploited so far. Still, this is one of the most promising aspects of these anions as it provides the opportunity to design molecular materials coupling optical activity and conductivity. In fact, in these two-network materials the chirality of the inorganic anions will induce chirality in the crystal lattice, leading therefore to chiral conducting materials [53]. The interest in chiral conductors has been recently highlighted since, in addition to the optical properties that would be present due to the chirality of the system, new phenomena has been predicted, namely electrical magneto-chiral anisotropy [54]. This effect should be observed in the magneto-transport properties of the material. While in a non chiral conductor the resistance has an even (quadratic) dependence on the external magnetic field (proportional to H^2), in a chiral conductor a new term arises that depends on the product between the external magnetic field and the current through the conductor, $I \times H$. In fact, the electrical resistance, *R*, is expected to have different values upon reversal of both the direction of the current, and that of the external magnetic field, i.e., when *I* changes to $-I$, or *H* to $-H$. The electrical magneto-chiral anisotropies observed thus far are quite small but it has been pointed out that they may be interesting in spintronics since in chiral conductors electrical resistance depends not only on the magnitude of spin polarization, but also on its direction.

Although salts formed by a pure enantiomer of the $[H_4Co_2Mo_{10}O_{38}]^{6-}$ and ET have not been reported so far, the racemic mixture of this polyanion leads to the salt **64** with a donor:anion stoichiometry of 9:1 [55]. Its consists of alternating organic and inorganic layers parallel to the *bc* plane (Fig. 10a). The organic layers are made of two crystallographically independent ET molecules (A and B) which form eclipsed stacks parallel to the *b* axis. Each stack is formed by only A or B molecules in such a way that two stacks made up of A-type molecules alternate with one stack made up of only B-type molecules. The organic layers adopt and unusual packing in which the donors of three adjacent stacks are parallel and form and angle of 54° with the donors of the next three stacks (Fig. 10b). Therefore, the organic sublattice of salt **64** presents features of the well-known α and β packing architectures. The inorganic layers are formed by stacks of POMs parallel to the *b* axis. Each of these polyanion stacks is formed by only one enantiomer and alternates with stacks composed of the other enantiomer. Therefore, the most interesting feature of this structure is that each of these inorganic stacks lies near three consecutive organic stacks having the ET molecular planes all parallel, while the three next neighbouring organic stacks lie near the inorganic stack made of POMs having the reverse chirality. Then, in this salt the unusual packing of the organic sublattice has likely been induced by the chirality of the POMs which could have been mediated through short contacts of the type C – H · · · O between the organic and inorganic sublattice (these contacts range between 2.44 and 3.10 Å). Concerning the electrical properties, salt **64** is a semiconductor with a room temperature conductivity of $9\,S\,cm^{-1}$ and a small activation energy of 40 meV.

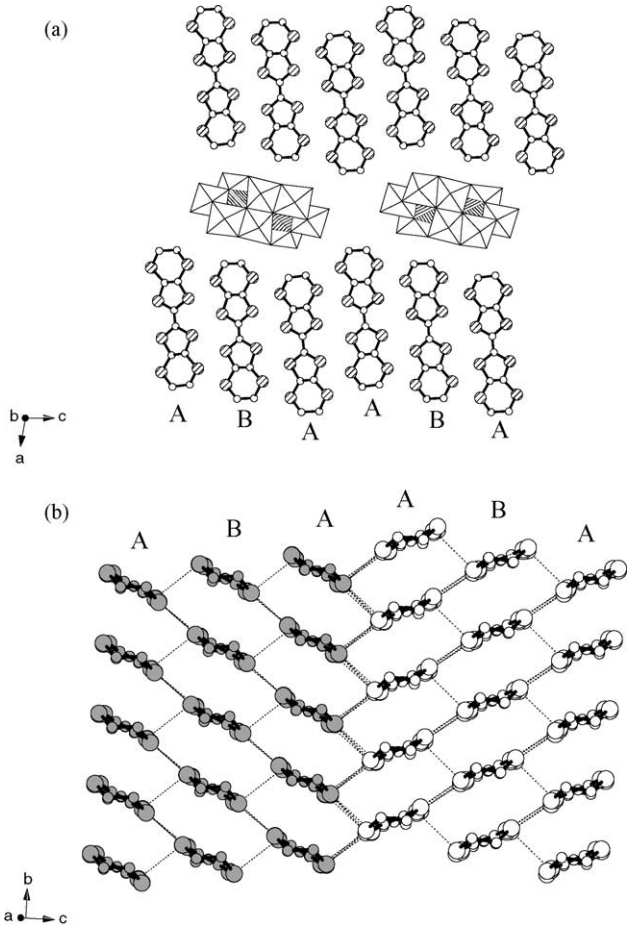

Fig. 10. (a) Projection of the structure of the radical salt **64** along the *b* axis. The carbon atoms are depicted as white spheres and the sulphur atoms as hatched spheres. (b) View of the organic layer of compound **64** along the long molecular axis of the ET molecules. Dotted lines represent S · · · S intermolecular contacts shorter than the sum of the van der Waals radii (3.60 Å). The crystallographically independent ET molecules of type A and B are depicted in grey and white color, respectively.

4. Molecular conductors based on other organic donors

4.1. Salts with perylene

The perylene donor (Fig. 1l) is one of the most frequently used donors in the preparation of highly conducting organic solids [35a]. In fact, perylene (per) has been used to produce many cation-radical salts with simple inorganic monoanions (such as Br^- [56], I^- [57], ClO_4^- [58], PF_6^- and AsF_6^- [59], etc.) and some magnetic anions ($FeCl_4^-$, $FeBr_4^-$, $M(mnt)^-$; M = Au, Co, Cu, Fe, Ni, Pd, Pt; mnt = maleonitriledithiolate) [60]. For these salts, high electrical conductivities at room temperature (up to 1400 S cm^{-1}) have been measured in some cases. A general feature of perylene salts is their one-dimensional electronic character due to the absence of atoms on the perylene molecule that can allow for in-plane interactions. It is interesting to combine POM anions with the perylene donor, because the distinctive geometries and big volumes of these anions can induce different packing patterns of the organic molecules, while their charges can influence the oxidation degree of the donors. All this would affect the transport properties of the resulting radical cation salts.

The first cation-radical salts of perylene and POMs have been prepared recently, using Lindqvist and Keggin polyanions. Three different Lindqvist polyanions have been used, namely $[Mo_6O_{19}]^{2-}$, $[W_6O_{19}]^{2-}$ and $[VW_5O_{19}]^{3-}$, which have given rise to three radical salts formulated as $(per)_5$[Lindqvist] (salts **65**, **66** and **67**, respectively) [31]. The crystal structures of the three compounds are very similar. There is an organic layer parallel to the *ac* plane which is made up of perylene chains running along the *c* direction (Fig. 11). The chains contain two types of crystallographically independent perylene molecules (A and B) which pack forming dimers with the sequence . . ., AABB, ... The dimers are almost eclipsed but there is a tilt angle of ∼40° between the AA and the BB dimers. The organic layers alternate with mixed layers formed by polyanions and isolated perylene molecules (of type C). This kind of structure had never been observed in any radical salt with perylene and shows, once more, the ability of POMs to induce novel structural types in the organic sublattices of organic radicals.

The intradimer distances are very similar in the AA (3.39 Å in **65** and 3.32 Å in **67**) and in the BB dimers (3.48 Å in **65** and 3.41 Å in **67**) and these are also very close to the interdimer distances (3.35 Å in **65** and 3.38 Å in **67**). Therefore, the size and the shape of the anion are the key factors determining the packing in the three salts, even if the anionic charge is different (−2 in **65** and **66**, and −3 in **67**). The only appreciable, but very important, effect of the anionic charge deals with the charge distribution in the organic sublattice. Thus, while the isolated perylene molecule C remains neutral, the stacked perylene molecules A and B have an average oxidation state of $(per)_4^{2+}$ in **65** and **66**, and $(per)_4^{3+}$ in **67**. This difference in the charge distribution accounts for the big differences observed in the physical properties of these

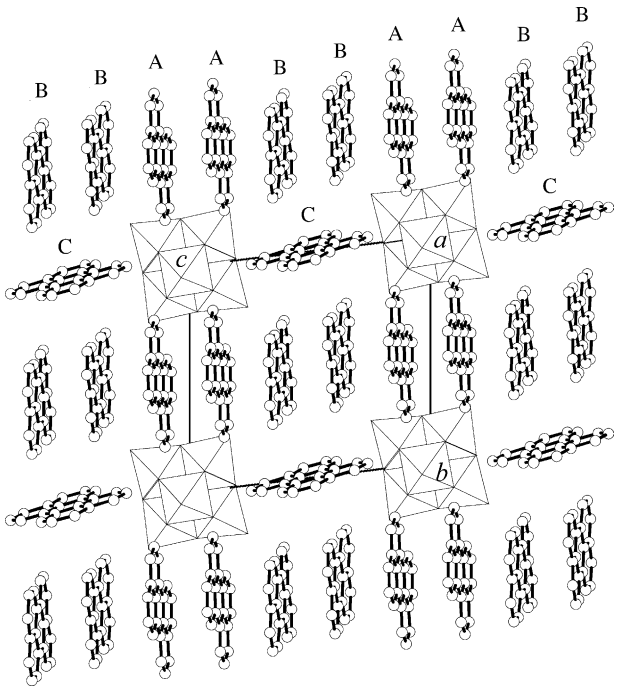

Fig. 11. View along the *a* axis of the alternating layers of compounds **65**, **66** and **67**. Carbon atoms are represented as white spheres.

salts. In fact, the salts with the dianionic Lindqvist POMs are diamagnetic and semiconductors with low room temperature conductivities (0.2 and 0.8 S cm^{-1} for **65** and **66**, respectively) and high activation energies (194 and 212 meV for **65** and **66**, respectively), and show positive Seebeck coefficients in the thermopower measurements (610 and 230 μS K^{-1} for **65** and **66**, respectively; see Fig. 12). In contrast, **67** contains the trianionic Lindqvist POM and is paramagnetic with one unpaired electron and semiconductor (Fig. 12) but with a higher room temperature conductivity (3 S cm^{-1}), a lower activation energy (129 meV) and a negative Seebeck coefficient (−350 μS K^{-1}). Hence, the use of POMs having the same geometry but different charges, has enabled the control of the electronic band filling in the resulting perylene salts and therefore, the tunning of the physical properties.

The Keggin anions $[PMo_{12}O_{40}]^{3-}$ and $[SiW_{12}O_{40}]^{4-}$ have also been combined with perylene [32]. Three different cation-radical salts have been obtained, namely $(per)_6[PMo_{12}O_{40}]\cdot CH_2Cl_2$ (salt **68**), $(per)_6[PMo_{12}O_{40}]\cdot CH_3CN$ (salt **69**) and $(per)_9(TBA)_4[SiW_{12}O_{40}]_2$ (salt **70**). Salts **68** and **69** are isostructural and show seven crystallographically independent perylene molecules, named A through G. The Keggin polyanions form an approximately simple-primitive-cubic lattice which leaves large rhombohedral cavities in which the perylene molecules form one-dimensional π-stacks parallel to the *a* axis (Fig. 13a). There are two different kinds of organic stacks both having a repeat unit of four molecules following the sequences . . ., BAAB, . . . in one chain and . . ., CDDC, . . . in the other chain. The perylene units in different stacks form an angle of about 9.5°. The other perylene molecules of type E, F and G are iso-

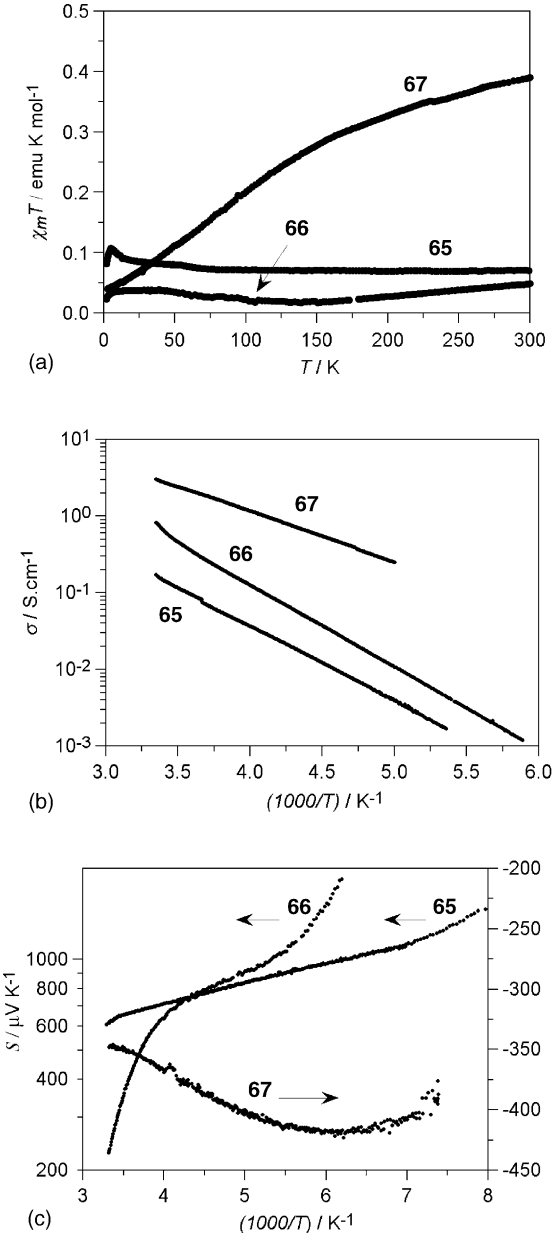

Fig. 12. (a) Thermal variation of the $\chi_m T$ product, (b) plot of the logarithm of the electrical conductivity vs. 1000/T and (c) plot of the Seebeck coefficient vs. 1000/T for salts **65**, **66** and **67**.

lated and separate the organic stacks (Fig. 13b). The structure of salt **70** is very different from that of the previous salts. In this compound the Keggin anions pack in a pseudo face-centred tetragonal lattice forming channels that are occupied by chains of perylene molecules or TBA^+ cations that come from the starting salt (Fig. 14). There are five types of perylene molecules named A through E. The first three form chains along the *c* axis following the sequence . . ., CBAAB, . . ., while the other D and E molecules are almost orthogonal, isolated and located between the POMs.

The three perylene salts containing Keggin anions behave as semiconductors although each one shows different char-

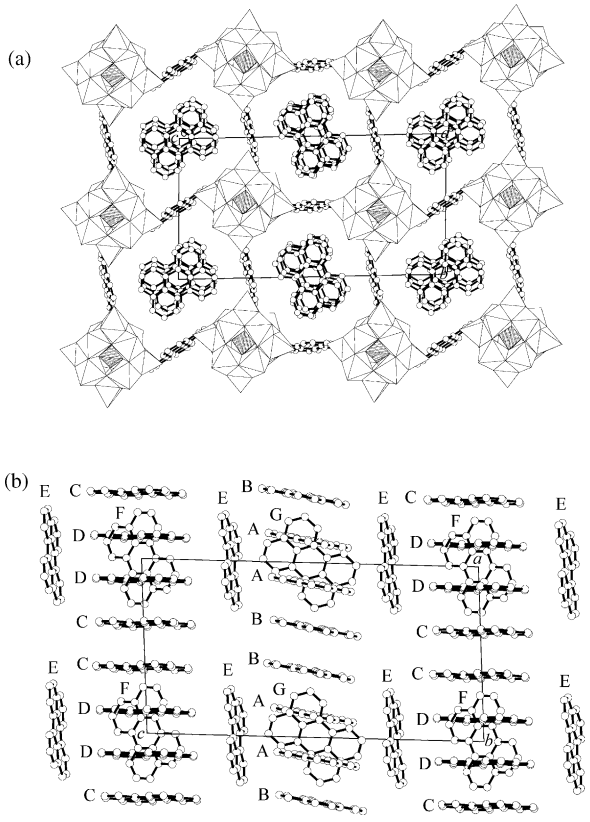

Fig. 13. (a) View of the structure of compounds **68** and **69** along the *a* axis. (b) View of the organic sublattice of **68** and **69** along the *b* axis including the labelling of the seven crystallographically different perylene molecules. Carbon atoms are represented as white spheres.

acteristics. The conductivity measurements for **68** indicate that this compound is a semiconductor with a room temperature conductivity of 69 S cm^{-1}. Interestingly, two distinct semiconducting regimes are observed which are separated by a structural phase transition at ∼150 K leading to an abrupt decrease in conductivity (Fig. 15a). The thermoelectric power measurements show a plateau of the Seebeck

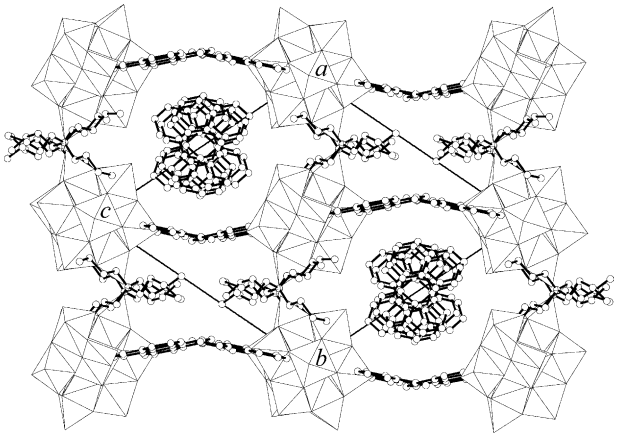

Fig. 14. Projection of the structure of compound **70** in the *ab* plane. The carbon atoms are depicted as white spheres and the nitrogen atoms as crossed spheres.

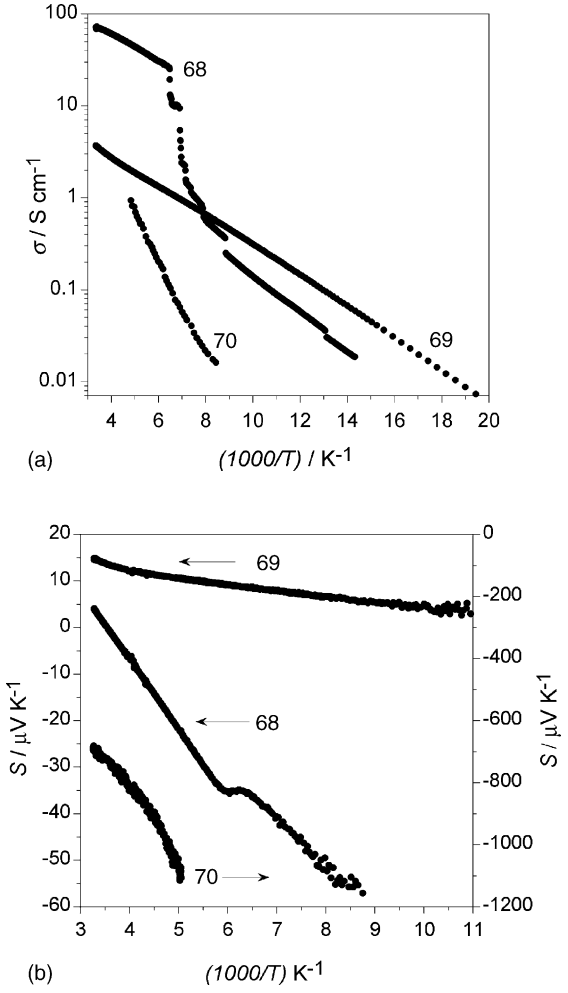

Fig. 15. Plots of the logarithm of the electrical conductivity (a) and the Seebeck coefficient (b) vs. 1000/*T* for the salts **68**, **69** and **70**.

coefficient at this temperature (Fig. 15b) confirming the existence of a subtle structural transition that originates microcracks in the crystals. Therefore, at temperatures higher than ∼150 K a semiconducting behavior with low activation energy (28.5 meV) and identical electron and hole mobilities is observed, while below this temperature the salt becomes more insulating, with a higher activation energy (40.8 meV). The conductivity of **69**, isostructural to **68**, is lower (3.6 S cm^{-1} at room temperature) and does not present any abrupt change upon cooling. The conductivity decreases monotonically when cooling down with an activation energy of 32 meV. The Seebeck confficient is positive in all the temperature range, with small values ranging from 14.9 μS K^{-1} at room temperature to 4.9 μS K^{-1} at 100 K. The positive values indicate hole dominated electrical conduction. **70** is a semiconductor with a lower room temperature conductivity (0.85 S cm^{-1}) and a much higher activation energy (101 meV), indicating the presence of a larger gap. The Seebeck coefficient is negative in all the temperature range and its fast decrease, approximately as 1/*T*, is typical of a semiconductor.

The magnetic susceptibility measurements of the three compounds indicate a complete pairing of the electrons in the perylene chains, even at room temperature. In contrast with what has been observed with the TTF-type donors, with perylene the phosphomolybdate Keggin anion is not reduced.

4.2. Salts with the seleno-substituted organic donors BEST and BETS

Seleno-substituted organic donors related to the ET molecule have attracted much interest in the field of the molecular conductors, as they offer a means of increasing the electrical conductivities thanks to the more extended 4d orbitals of the selenium, which enhance the donor–donor overlaps [3c].

Two different seleno-substituted donors derivatives of the ET molecule have been combined with POMs, namely BEST and BETS (Fig. 1i and j). However, whereas ET has been successfully combined with many different Keggin polyoxoanions to give extensive series of crystalline radical salts, the POM salts with seleno-substituted donors have been much more difficult to obtain. Actually, only two different cation-radical salts could be structurally characterized with the Keggin polyoxomolybdates $[PMo_{12}O_{40}]^{3-}$ and $[SMo_{12}O_{40}]^{2-}$; with other POMs only black crystalline powders have been obtained. The two radical salts are formulated as $[BEDS\text{-}TTF]_3H[PMo_{12}O_{40}]\cdot CH_3CN\cdot CH_2Cl_2$ (**74**) and α_1-$[BEDT\text{-}TSF]_8[SMo_{12}O_{40}]$ (**75**). The crystal structure of **74** [29] is quite unusual since, although it presents a layered structure, the two kinds of organic layers present in this structure penetrate into the inorganic layers to afford a quasi 3D organic packing with several short intra and interlayer contacts involving mainly the selenium atoms (Fig. 16). Another unusual feature of this structure is the fact that the Keggin anions are not disordered, as occurs in most of the salts of this anions with bulky, non polarising, cations [61]. The short donor-anions interactions (the shortest Se···O, S···O and C···O distances are 2.95, 2.96 and 3.02 Å, respectively) may account for this observation. EPR and magnetic measurements show that in this salt the $[PMo_{12}O_{40}]^{4-}$ anion is reduced by one electron, which is delocalized at high temperatures but trapped at low temperatures. Moreover, the radical donors are fully oxidized, accounting for the insulating nature of this salt. Therefore, a small modification in the ET molecule (such as the substitution of S by Se in the periphery) has led to a drastic change in the composition or the resulting radical salts (from a stoichiometry 8:1–3:1) and, therefore, in its structure and electronic properties.

In contrast, when the BETS donor (in which the inner S atoms of ET are substituted by Se atoms) is combined with the Keggin anion $[SMo_{12}O_{40}]^{2-}$, compound **75** is obtained [33] which is isostructural to the α_1 family previously described. This recent result allows for the comparison of the two isostructural salts containing the $[SMo_{12}O_{40}]^{2-}$ polyanion and ET (salt **37**) or BETS (salt **75**), providing a way to evaluate the influence of the seleniated donor on the

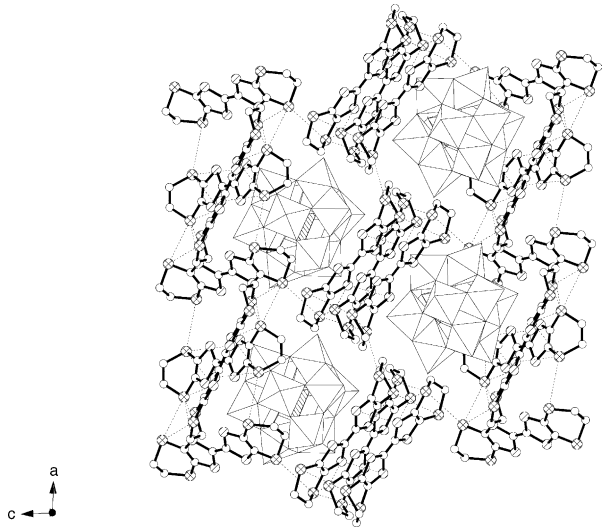

Fig. 16. View along the *b* axis of the structure of compound **74** showing the interpenetrated layers of POMs and BESTs. The carbon atoms are depicted as white spheres, the sulphur atoms as hatched spheres, and the selenium atoms as crossed spheres. Dotted lines represent S···S, Se···Se and Se···S intermolecular contacts shorter than the sum of the van der Waals radii.

physical properties of these hybrids. Although only a preliminary characterization has been performed, EPR measurements indicate that the $[SMo_{12}O_{40}]^{2-}$ polyanion has been reduced by two electrons and therefore has a charge of −4 in both radical salts. These are the first examples of TTF-type radical salts in which the POM has been reduced by two electrons. This is probably due to the low reduction potential of the $[SMo_{12}O_{40}]^{2-}$ polyanion [62]. The conductivity properties of compounds **37** and **75** are slightly different (Fig. 17). While **37** exhibits the typical semiconducting behavior shown by all the members of the α_1 family of ET salts with Keggin anions, **75** exhibits a metallic behavior in the intermediate region of temperatures (in between 200 and 60 K). Below 60 K the semiconducting behavior is restored and the conductivity values decrease quickly. The larger electron delocalization

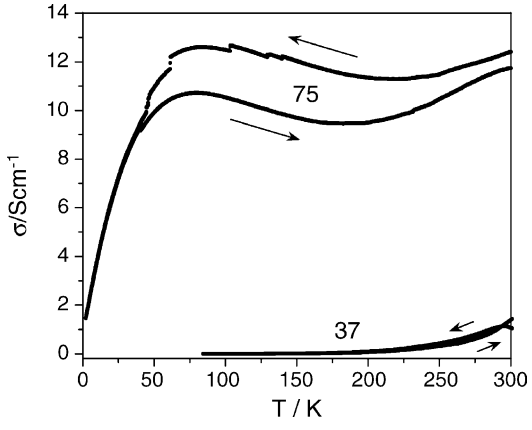

Fig. 17. Temperature dependence of the electrical conductivity (σ) of compounds **37** and **75**. The measurements were made initially decreasing and afterwards raising the temperature (see arrows).

observed in the selenium derivative seems to be in agreement with the expectations provided by the more extended 4d orbitals of the selenium atoms, which enhance the donor–donor overlaps.

4.3. Salts with the oxygen-substituted organic donor BEDO

The oxygenated donor BEDO (Fig. 1k) is an interesting candidate to be combined with POMs, as most radical salts containing this donor are molecular metals, including two superconductors: $[BEDO]_3[Cu_2(NCS)_3]$ [35c] and $[BEDO]_2[ReO_4]\cdot H_2O$[35d,35e]. Moreover, BEDO-TTF could establish stronger intermolecular interactions (of the type O···O) with the metal-oxide clusters than the classical sulfur-containing donors.

The first POM-containing radical salt with BEDO has recently been reported [63]. It can be formulated as $[BEDO]_6K_2[BW_{12}O_{40}]\cdot 11H_2O$ (salt **76**) and its crystal structure consists of alternating layers of organic donors and inorganic POMs (Fig. 18a). The organic layers adopt the so-called β″ packing arrangement [43] (Fig. 18b) with numerous short intermolecular S···S and S···O separations (less than 3.60 and 3.32 Å, respectively). These layers are made up of three crystallographically independent BEDO molecules (A–C) which arrange forming very uniform stacks following the sequence . . ., ABC, . . . in one chain, and the opposite one (. . ., CBA, . . .) in the adjacent chains. All three independent molecules have the same geometry and similar intramolecular bond lengths and angles. It underlines the marked tendency of BEDO to form very uniform β packing architectures as a result of the strong intermolecular S···S and S···O interactions within the organic network, even in the presence of the POM network. This is a noteworthy difference with respect to the other radical salts of Keggin anions with the related donors ET, BEST or BETS, in which the inorganic network often induces organic networks wherein the organic molecules have very different conformations, geometries and charges, and form very irregular and exotic stacks, or even lose the typical 2D packing architectures.

The inorganic layers are formed by the Keggin anions and the K^+ cations, that come from the reagent salt, filling the cavities or voids existing between the POMs. In the other Keggin-based radical salts the organic donors fill these voids by "docking" of the outer ethylene groups into the cavities provided by the inorganic network. This feature is often one of the reasons leading to irregular stacks of the donors, as we have previously described in this review. In compound **76** the insertion of K^+ ions is related to the formation of fully eclipsed stacks of BEDO units which can not fill the cavities created in the inorganic sublattice. Actually, the K^+ ions play an essential role in stabilizing the structure of this salt. In fact, in the absence of K^+, electro-oxidation of BEDO in presence of $[BW_{12}O_{40}]^{5-}$ does not afford any product on the electrode. The conductivity measurements of **76** reveals a metallic character across the studied temper-

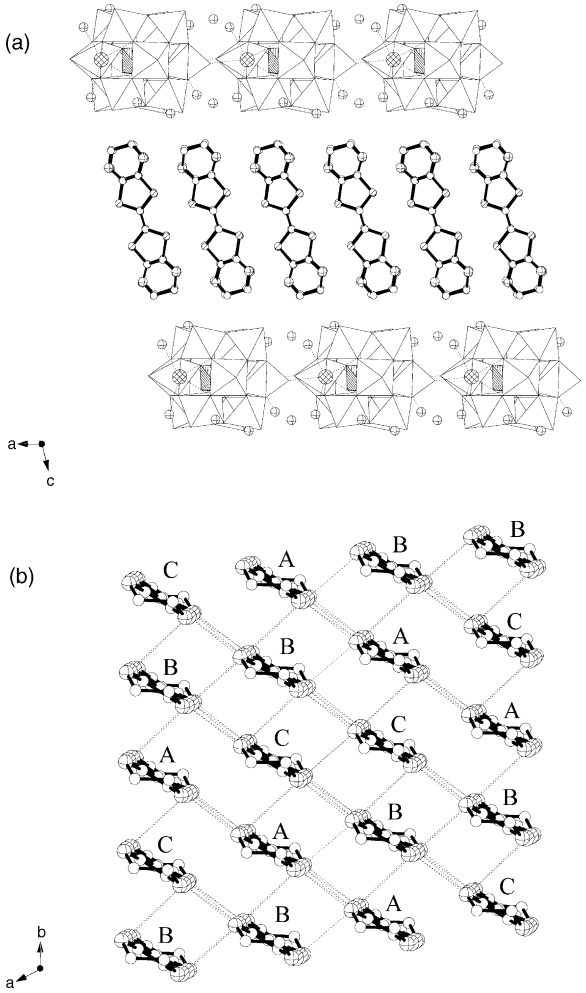

Fig. 18. (a) Structure of the radical salt **76** showing the alternating layers of the POMs and the organic donors. The carbon atoms are depicted as white spheres, the sulphur atoms as hatched spheres, the oxygen atoms as small crossed spheres and the potassium ions as bigger crossed spheres. Dotted lines represent the coordination of the potassium ions by water molecules or oxygen atoms of the POMs. (b) View of the organic layer of compound **76** along the *c* axis, showing the β″ type of packing. Dotted lines represent S···S and S···O intermolecular contacts shorter than the sum of the van der Waals radii.

ature range (300–2 K, see Fig. 19). The room temperature conductivity is about 37 S cm^{-1} and gradually increases as the temperature is decreased to reach a maximum value of 910 S cm^{-1} at 2 K. The temperature dependence of the resistivity shows a linear dependence from room temperature to 200 K, which is usually associated with electron–phonon scattering. Below this temperature the resistivity is proportional to T^2 (inset in Fig. 19), typical of metallic organic salts where electron–electron scattering in the dominant mechanism of conductivity. Compound **76** is the first example of a POM-containing radical salt that exhibits a metallic behavior down to 2 K. This result demonstrates that it is possible to use bulky and highly charged polyoxoanions as components of new radical salts that behave as a metal and opens up the possibility of synthesizing new molecular materials

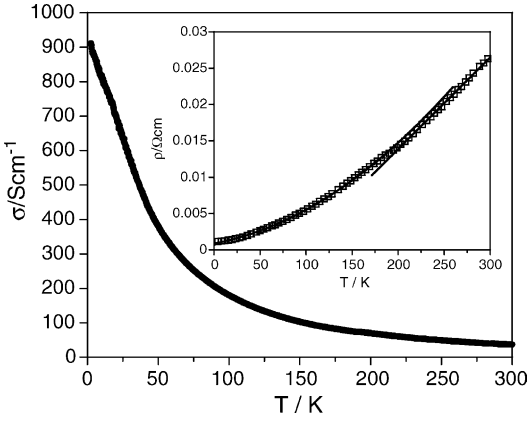

Fig. 19. Thermal variation of the conductivity (σ) of compound **76** showing the metallic behavior down to 2 K. The inset shows the plot of the thermal variation of the resistivity (ρ) and the solid lines show the linear and quadratic dependencies of ρ above and below 200 K, respectively.

with coexisting, or even coupling, conducting electrons and localized magnetic moments. The synthetic strategy simply consists in combining the BEDO donor with inorganic layers of magnetic Keggin POMs and K^+ ions. This would give rise to a new series of molecular materials, similar to the reported series with the ET donor, but with the advantage of having a metallic behavior down to very low temperatures.

5. Concluding remarks

In this review we have highlighted the recent advances reported in the interface between polyoxometalate complexes and molecular conductors. POM-containing radical salts have demonstrated that POMs can induce novel and very different packing motifs in the organic sublattice of these hybrid molecular materials. Besides the structural effects induced by these large inorganic anions in the organic network, POMs have shown to provide hybrid materials with interesting electronic properties. In fact, these molecular metal oxide clusters have been successfully used not only in the synthesis of many molecular semiconductors, but also to obtain metallic-like salts with broad metal–semiconductor transitions, and even a molecular metal showing metallic conductivity down to 2 K.

On the other hand, they have also allowed us to combine localized magnetic moments, delocalized electrons and even magnetic clusters, with the delocalized electrons of the organic sublattice, leading to materials with coexistence of magnetic and conducting properties. Still, in all the reported examples the two electronic networks behave in an independent way. One of the reasons that accounts for this lack of interaction is the poor conductivity of the materials at low temperatures. The recent preparation of a POM-containing molecular metal showing a large electron delocalization at low temperatures constitutes a promising result in this context and needs to be exploited.

Finally, the unusual ability displayed by some POMs of changing their anionic charge while keeping the size and shape, has also started to be exploited to tune the magnetic and electrical properties in isostructural series of compounds. Other abilities of POMs, as for example the chiral properties of some of them, need still to be exploited.

The examples reported here have shown the great potential offered by these coordination complexes in the area of functional molecular materials and the progress that still remains to be done. Note that this application of POM chemistry is very recent. In fact, most of the examples have been reported in the last decade. This development is not limited to crystals. Hybrid films containing POMs also constitute an active focus of interest in materials chemistry [12j,64].

Acknowledgements

Financial support from the Spanish Ministerio de Educación y Ciencia (MEC) (MAT2004-03849) and the Generalitat Valenciana is acknowledged. CGS thanks the MEC for a research contract (Programa Ramón y Cajal).

References

[1] L.R. Melby, Can. J. Chem. 43 (1965) 148.
[2] (a) J. Ferraris, D.O. Cowan, V.V. Walatka, J.H. Perlstein Jr., J. Am. Chem. Soc. 95 (1973) 948;
(b) L.B. Coleman, M.J. Cohen, D.J. Sandman, F.G. Yamagishi, A.F. Garito, A.J. Heeger, Solid State Commun. 12 (1973) 1125.
[3] (a) A. Andrieux, C. Duroure, D. Jérome, K. Bechgaard, J. Phys. Lett. 40 (1979) 381;
(b) D. Jérome, A. Mazaud, M. Ribault, K. Bechgaard, J. Phys. Lett. 41 (1980) 195;
(c) J.M. Williams, J.R. Ferraro, R.J. Thorn, K.D. Carlson, U. Geiger, H.H. Wang, A.M. Kini, M.H. Whangbo, in: R.N. Crimes (Ed.), Organic Superconductors: Synthesis, Structure, Properties and Theory, Prentice Hall, Englewood Cliffs, NJ, 1992.
[4] P. Day, Philos. Trans. R. Soc. Lond. A314 (1985) 145.
[5] (a) A.V. Gudenko, V.B. Ginodman, V.E. Korotkov, A.V. Koshelap, N.D. Kushch, V.N. Laukhin, L.P. Rozenberg, A.G. Khomenko, R.P. Shibaeva, E.B. Yagubskii, in: G. Saito, G. Kagoshima (Eds.), The Physics and Chemistry of Organic Superconductors, Springer Verlag, Berlin, Germany, 1990;
(b) R.P. Shibaeva, V.E. Korotkov, L.P. Rozenberg, Sov. Phys. Crystallogr. 36 (1991) 820;
(c) M. Kurmoo, T. Mallah, L. Marsden, M. Allan, R.H. Friend, F.L. Pratt, W. Hayes, D. Chasseau, G. Bravic, L. Ducasse, P. Day, J. Am. Chem. Soc. 114 (1992) 10722.
[6] M. Kurmoo, A.W. Graham, P. Day, S.J. Coles, M.B. Hursthouse, J.M. Caulfield, J. Singleton, L. Ducasse, P. Guionneau, J. Am. Chem. Soc. 117 (1995) 12209.
[7] H. Kobayashi, H. Tomita, T. Naito, A. Kobayashi, F. Sakai, T. Watanabe, P. Cassoux, J. Am. Chem. Soc. 118 (1996) 368.
[8] E. Coronado, J.R. Galán-Mascarós, C.J. Gómez-García, V.N. Laukhin, Nature 408 (2000) 447.
[9] E. Coronado, P. Day, Chem. Rev. 104 (2004) 5419.
[10] (a) L. Ouahab, M. Bencharif, D. Grandjean, C.R. Acad. Sci. Paris Ser. II 307 (1988) 749;
(b) L. Ouahab, D. Grandjean, M. Bencharif, Acta Crystallogr. C47 (1991) 2670.
[11] E. Coronado, C.J. Gómez-García, Chem. Rev. 98 (1998) 237.
[12] Several reviews have described the progress made by the combination of polyoxometalates with organic donor molecules:;
(a) E. Coronado, C.J. Gómez-García, in: M.T. Pope, A. Müller (Eds.), Polyoxometalates: from Platonic Solids to Anti-retroviral Activity, Kluwer Academic Publishers, 1994, p. 233;
(b) L. Ouahab, in: M.T. Pope, A. Müller (Eds.), Polyoxometalates: from Platonic Solids to Anti-retroviral Activity, Kluwer Academic Publishers, 1994, p. 245;
(c) E. Coronado, C.J. Gómez-García, Comments Inorg. Chem. 17 (1995) 255;
(d) E. Coronado, J.R. Galán-Mascarós, C. Giménez-Saiz, C.J. Gómez-García, in: O. Khan (Ed.), Magnetism: A Supramolecular Function, NATO ASI Series, vol. C484, Kluwer Academic Publishers, 1996, p. 281;
(e) E. Coronado, P. Delhaès, J.R. Galán-Mascarós, C. Giménez-Saiz, C.J. Gómez-García, Synth. Met. 85 (1997) 1647;
(f) L. Ouahab, Chem. Mater. 9 (1997) 1909;
(g) E. Coronado, J.R. Galán-Mascarós, C. Giménez-Saiz, C.J. Gómez-García, Adv. Mater. Opt. Electron. 8 (1998) 61;
(h) J.J. Borrás-Almenar, J.M. Clemente-Juan, M. Clemente-León, E. Coronado, J.R. Galán-Mascarós, C.J. Gómez-García, in: M.T. Pope, A. Müller (Eds.), Polyoxometalate Chemistry: From topology via self-assembly to applications, Kluwer Academic Publishers, 2001, p. 231;
(i) L. Ouahab, S. Golhen, in: M.T. Pope, A. Müller (Eds.), Polyoxometalate Chemistry: From topology via self-assembly to applications, Kluwer Academic Publishers, 2001, p. 205;
(j) M. Clemente-León, E. Coronado, C. Giménez-Saiz, C.J. Gómez-García, in: J.J. Borrás-Almenar, E. Coronado, A. Müller, M. Pope (Eds.), Polyoxometalate Molecular Science, NATO Science Series, Kluwer Academic Publishers, 2003, p. 417.
[13] (a) A. Mhanni, L. Ouahab, O. Peña, D. Granjean, C. Garrigou-Lagrange, P. Delhaès, Synth. Met. 42 (1991) 1703;
(b) L. Ouahab, M. Bencharif, A. Mhanni, D. Pelloquin, J.F. Halet, O. Peña, J. Padiou, D. Grandjean, C. Garrigou-Lagrange, J. Amiell, P. Delhaès, Chem. Mater. 4 (1992) 666;
(c) D. Attanasio, C. Bellito, M. Bonamico, V. Fares, S. Patrizio, Synth. Met. 42 (1991) 2289;
(d) D. Attanasio, C. Bellito, M. Bonamico, G. Righini, G. Staulo, Mater. Res. Soc. Symp. Proc. 247 (1992) 545;
(e) C. Bellito, G. Staulo, R. Bozio, C. Pecile, Mol. Cryst. Liq. Cryst. 234 (1993) 205.
[14] (a) S. Triki, L. Ouahab, J. Padiou, D. Grandjean, J. Chem. Soc. Chem. Commun. (1989) 1068;
(b) S. Triki, L. Ouahab, J.F. Halet, O. Peña, J. Padiou, D. Grandjean, C. Garrigou-Lagrange, P. Delhaès, J. Chem. Soc., Dalton Trans. (1992) 1217;
(c) C. Bellito, D. Attanasio, M. Bonamico, V. Fares, P. Imperatori, S. Patrizio, Mater. Res. Soc. Symp. Proc. 173 (1990) 143;
(d) D. Attanasio, C. Bellito, M. Bonamico, V. Fares, P. Imperatori, Gazz. Chim. Ital. 121 (1991) 155.
[15] S. Triki, Ph.D. thesis, University of Rennes, 1992.
[16] S. Triki, L. Ouahab, D. Grandjean, Acta Cryst. C49 (1991) 132.
[17] (a) S. Triki, L. Ouahab, D. Grandjean, J.M. Fabre, Acta Cryst. C47 (1991) 1371;
(b) S. Triki, L. Ouahab, D. Grandjean, J. Amiel, C. Garrigou-Lagrange, P. Delhaès, J.M. Fabre, Synth. Met. 42 (1991) 2589;
(c) S. Triki, L. Ouahab, Acta Cryst. C50 (1994) 219;
(d) E. Coronado, S. Curreli, J. M. Fabre, C. Giménez-Saiz, C. J. Gómez-García, manuscript in preparation.
[18] (a) A. Speghini, D. Pedron, C. Bellito, L. Feltre, R. Bozio, Mol. Cryst. Liq. Cryst. 234 (1993) 219;
(b) S. Kruszewski, L. Feltre, R. Bozio, C. Bellito, Acta Phys. Pol. A 83 (1993) 431.
[19] (a) C.J. Gómez-García, E. Coronado, S. Triki, L. Ouahab, P. Delhaès, Adv. Mater. 5 (1993) 283;

(b) C.J. Gómez-García, E. Coronado, S. Triki, L. Ouahab, P. Delhaès, Synth. Met. 56 (1993) 1787.
[20] E. Coronado, S. Curreli, C. Giménez-Saiz, C. J. Gómez-García, manuscript in preparation.
[21] S. Triki, L. Ouahab, D. Grandjean, Acta Cryst. C74, 645.
[22] S. Triki, L. Ouahab, D. Grandjean, R. Canet, C. Garrigou-Lagrange, P. Delhaès, Synth. Met. 56 (1993) 2028.
[23] L. Ouahab, S. Golhen, S. Triki, A. Łapiński, M. Golub, R. Świetlik, J. Cluster Sci. 13 (2002) 267.
[24] M. Kurmoo, M. Bonamico, C. Bellito, V. Fares, F. Federici, P. Guionneau, L. Ducasse, H. Kitagawa, P. Day, Adv. Mater. 10 (1999) 545.
[25] (a) A. Davidson, K. Boubekour, A. Pénicaud, P. Auban, C. Lenoir, P. Batail, G. Hervé, J. Chem. Soc., Chem. Commun. (1989) 1373;
(b) C.J. Gómez-García, L. Ouahab, C. Giménez-Saiz, S. Triki, E. Coronado, P. Delhaès, Angew. Chem. Int. Ed. Engl. 33 (1994) 223;
(c) C.J. Gómez-García, C. Giménez-Saiz, S. Triki, E. Coronado, P. Le Magueres, L. Ouahab, L. Ducasse, C. Sourisseau, P. Delhaès, Inorg. Chem. 34 (1995) 4139;
(d) C.J. Gómez-García, C. Giménez-Saiz, S. Triki, E. Coronado, L. Ducasse, P. Le Magueres, L. Ouahab, P. Delhaès, Synth. Met. 70 (1995) 783;
(e) C. Bellitto, M. Bonamico, G. Staulo, Mol. Cryst. Liq. Cryst. 232 (1993) 155;
(f) M. Kurmoo, P. Day, C. Bellito, Synth. Met. 70 (1995) 963;
(g) C. Bellitto, M. Bonamico, V. Fares, F. Federici, G. Righini, M. Kurmoo, P. Day, Chem. Mater. 7 (1995) 1475;
(h) J. Peng, E. Wang, M. Xin, J. Liu, Y. Zhou, W. Li, Polyhedron 18 (1999) 3147.
[26] (a) J.R. Galán-Mascarós, C. Giménez-Saiz, S. Triki, C.J. Gómez-García, E. Coronado, L. Ouahab, Angew. Chem. Int. Ed. Engl. 34 (1995) 1460;
(b) E. Coronado, J.R. Galán-Mascarós, C. Giménez-Saiz, C.J. Gómez-García, S. Triki, P. Delhaès, Mol. Cryst. Liq. Cryst. 274 (1995) 89;
(c) E. Coronado, J.R. Galán-Mascarós, C. Giménez-Saiz, C.J. Gómez-García, S. Triki, J. Am. Chem. Soc. 120 (1998) 4671.
[27] (a) E. Coronado, J.R. Galán-Mascarós, C. Giménez-Saiz, C.J. Gómez-García, V.N. Laukhin, Adv. Mater. 8 (1996) 801;
(b) C. Giménez-Saiz, J.D. Woollins, A.M.Z. Slawin, E. Coronado, J.M. Martínez-Agudo, C.J. Gómez-García, N. Robertson, Mol. Cryst. Liq. Cryst. 335 (1999) 43;
(c) E. Coronado, M. Clemente-León, J.R. Galán-Mascarós, C. Giménez-Saiz, C.J. Gómez-García, E. Martínez-Ferrero, J. Chem. Soc., Dalton Trans. (2000) 3955.
[28] M. Clemente-León, E. Coronado, J.R. Galán-Mascarós, C. Giménez-Saiz, C.J. Gómez-García, T. Fernández-Otero, J. Mater. Chem. 8 (1998) 309.
[29] E. Coronado, J.R. Galán-Mascarós, C. Giménez-Saiz, C.J. Gómez-García, L.R. Falvello, P. Delhaès, Inorg. Chem. 37 (1998) 2183.
[30] E. Coronado, J.R. Galán-Mascarós, C. Giménez-Saiz, C.J. Gómez-García, C. Rovira, J. Tarrés, S. Triki, J. Veciana, J. Mater. Chem. 8 (1998) 313.
[31] M. Clemente-León, E. Coronado, C. Giménez-Saiz, C.J. Gómez-García, E. Martínez-Ferrero, M. Almeida, E.B. Lopes, J. Mater. Chem. 11 (2001) 2176.
[32] E. Coronado, J.R. Galán-Mascarós, C. Giménez-Saiz, C.J. Gómez-García, E. Martínez-Ferrero, M. Almeida, E.B. Lopes, S.C. Capelli, R.M. Llusar, J. Mater. Chem. 14 (2004) 1867.
[33] A. Alberola, E. Coronado, S. Curreli, C. Giménez-Saiz, C.J. Gómez-García, manuscript in preparation.
[34] I. Alonso, E. Coronado, S. Curreli, H. Degenbeck, C. Giménez-Saiz, C.J. Gómez-García, manuscript in preparation.
[35] (a) M. Almeida, R.T. Henriques, in: H.S. Nalwa (Ed.), Handbook of Organic Conductive Molecules and Polymers, vol. 1, John Wiley, Chichester, 1997, p. 87;
(b) S. Uji, H. Shinagawa, T. Terashima, T. Yakabe, Y. Terai, M. Tokumoto, A. Kobayashi, H. Tanaka, H. Kobayashi, Nature 410 (2001) 908;
(c) M.A. Beno, H.H. Wang, A.M. Kini, K.D. Carlson, U. Geiser, W.K. Kwok, J.E. Thompson, J.M. Williams, J. Ren, M.-H. Whangbo, Inorg. Chem. 29 (1990) 1599;
(d) S. Kahlich, D. Schweitzer, I. Heinen, S.E. Lan, B. Nuber, H.J. Keller, K. Winzer, H.W. Helberg, Solid State Commun. 80 (1991) 191;
(e) L.I. Buravov, A.G. Khomenko, N.D. Kushch, V.N. Laukhin, A.I. Schegolev, E.B. Yagubskii, L.P. Rozenberg, R.P. Shibaeva, J. Phys. I France 2 (1992) 529.
[36] M.T. Pope, A. Müller, Angew. Chem. Int. Ed. Engl. 30 (1991) 34.
[37] V.W. Day, W.G. Klemperer, D.J. Maltbie, J. Am. Chem. Soc. 109 (1987) 2991.
[38] (a) W.G. Klemperer, T.A. Marquat, O.M. Yagui, Angew. Chem. Int. Ed. Engl. 31 (1992) 49;
(b) A. Müller, F. Peters, M.T. Pope, D. Gatteschi, Chem. Rev. 98 (1998) 239.
[39] (a) A. Müller, R. Sessoli, E. Krickemeyer, H. Bögge, J. Meyer, D. Gatteschi, L. Pardi, J. Westphal, K. Hovemeier, R. Rohlfing, J. Döring, F. Hellweg, C. Beugholt, M. Schmidtmann, Inorg. Chem. 36 (1997) 5239;
(b) M.I. Khan, J. Zubieta, Angew. Chem. Int. Ed. Engl. 33 (1994) 49;
(c) J. Salta, Q. Chen, Y.D. Chang, J. Zubieta, Angew. Chem. Int. Ed. Engl. 33 (1994) 757.
[40] (a) A. Müller, M. Penk, E. Krickemeyer, H. Bögge, H.J. Walberg, Angew. Chem. Int. Ed. Engl. 27 (1988) 1719;
(b) L. Suber, M. Bonamico, V. Fares, Inorg. Chem. 36 (1997) 2030.
[41] (a) D. Gatteschi, L. Pardi, A.L. Barra, A. Müller, in: M.T. Pope, A. Müller (Eds.), Polyoxometalates: From Platonic Solids to Anti-Retroviral Activity, Kluwer Academic Publishers, Dordrecht, The Netherlands, 1994, p. 219;
(b) A.L. Barra, D. Gatteschi, L. Pardi, A. Müller, J. Döring, J. Am. Chem. Soc. 114 (1992) 8509;
(c) D. Gatteschi, L. Pardi, A.L. Barra, A. Müller, J. Döring, Nature 354 (1991) 463.
[42] E. Coronado, J.R. Galán-Mascarós, C. Giménez-Saiz, C.J. Gómez-García, E. Martínez-Ferrero, M. Almeida, E.B. Lopes, Adv. Mater. 16 (2004) 324.
[43] For an explanation on the different packing motifs adopted by the ET salts see:;
(a) T. Mori, Bull. Chem. Soc. Jpn. 71 (1998) 2509;
(b) T. Mori, H. Mori, S. Tanaka, Bull. Chem. Soc. Jpn. 72 (1999) 179.
[44] P. Guionneau, C.J. Kepert, G. Bravic, D. Chasseau, M.R. Truter, M. Kurmoo, P. Day, Synth. Met. 86 (1997) 1973.
[45] E. Martínez-Ferrero, Ph.D. thesis, University of Valencia, 2003.
[46] A. Łapiński, V. Starodub, M. Golub, A. Kravchenko, V. Baumer, E. Faulques, A. Graja, Synth. Met. 138 (2003) 483.
[47] (a) M. Kozik, C.F. Hammer, L.C.W. Baker, J. Am. Chem. Soc. 108 (1986) 2748;
(b) I. Kawafune, G. Matsubayashi, Chem. Lett. (1992) 1869.
[48] C. Bellito, M. Bonamico, J. Peng, Synt. Met. 85 (1997) 1583.
[49] E. Coronado, H. Degenbeck, C. Giménez-Saiz, C. J. Gómez-García, manuscript in preparation.
[50] H.T. Evans, M.T. Pope, Inorg. Chem. 23 (1984) 501.
[51] C.J. Kepert, M. Kurmoo, P. Day, Inorg. Chem. 36 (1997) 1128.
[52] L. Ouahab, S. Golhen, Y. Yoshida, G. Saito, J. Cluster Sci. 14 (2003) 193.
[53] (a) E. Coronado, J.R. Galán-Mascarós, J. Mater. Chem. 15 (2005) 66;
(b) E. Coronado, J.R. Galán-Mascarós, C.J. Gómez-García, A. Murcia-Martínez, E. Canadell, Inorg. Chem. 43 (2004) 8072.
[54] G.L.J.A. Rikken, J. Fölling, P. Wyder, Phys. Rev. Lett. 87 (2001) 236602.

[55] E. Coronado, S. Curreli, C. Giménez-Saiz, C. J. Gómez-García, J. Roth, Synth. Met., in press.
[56] H. Akamatu, H. Inokuchi, Y. Matsunaga, Bull. Chem. Soc. Jpn. 29 (1956) 213.
[57] H.C.I. Kao, M. Jones, M.M. Labes, J. Chem. Soc., Chem. Commun. (1979) 329.
[58] D. Schweiter, I. Henning, K. Bender, H. Endres, H.J. Keller, Mol. Cryst. Liq. Cryst. 120 (1985) 329.
[59] (a) H.J. Keller, D. Nöthe, H. Pritzkov, D. Wehe, M. Werner, P. Koch, D. Schweitzer, Mol. Cryst. Liq. Cryst. 62 (1980) 181;
(b) W. Brütting, W. Riess, Acta Phys. Pol. A 87 (1995) 785.
[60] (a) V. Gama, M. Almeida, R.T. Henriques, I.C. Santos, A. Domingos, S. Ravy, J.P. Pouget, J. Phys. Chem. 95 (1991) 4263;
(b) V. Gama, R.T. Henriques, G. Bonfait, L.C. Pereira, J.C. Waerenborgh, I.C. Santos, M.T. Duarte, J.M.P. Cabral, M. Almeida, Inorg. Chem. 31 (1992) 2598.
[61] (a) V.S. Sergienko, M.A. Porai-Koshits, E.N. Yurchenko, J. Struct. Chem. (Engl. Transl.) 21 (1980) 87;
(b) J. Fuchs, A. Thiele, R. Palm, Angew. Chem. Int. Ed. Engl. 21 (1982) 789;
(c) H.T. Evans, M.T. Pope, Inorg. Chem. 23 (1984) 501;
(d) D. Attanasio, M. Bonamico, V. Fares, P. Imperatori, L. Buber, J. Chem. Soc. Dalton Trans. (1990) 3221.
[62] A.M. Bond, D.C. Coomber, R. Harika, V.M. Hultgren, M.B. Rooney, T. Vu, A.G. Wedd, Electroanalysis 13 (2001) 1475.
[63] E. Coronado, C. Giménez-Saiz, C.J. Gómez-García, S.C. Capelli, Angew. Chem. Int. Ed. 43 (2004) 3022.
[64] (a) P. Gómez-Romero, M. Lira-Cantú, Adv. Mater. 9 (1997) 144;
(b) M. Clemente-León, E. Coronado, P. Delhaès, C.J. Gómez-García, C. Mingotaud, Adv. Mater. 13 (2001) 574;
(c) S. Cheng, T. Fernández-Otero, E. Coronado, C.J. Gómez-García, E. Martínez-Ferrero, C. Giménez-Saiz, J. Phys. Chem. B 106 (2002) 7585;
(d) T. Fernández-Otero, S.A. Cheng, E. Coronado, E. Martínez-Ferrero, C.J. Gómez-García, Chem. Phys. Chem. 9 (2002) 808;
(e) Q. Wu, X. Xie, Mat. Chem. Phys. 77 (2002) 621.
[65] K. Boubekeur, R. Riccardi, P. Batail, E. Canadell, C.R. Acad. Sci. Paris Ser. IIc 1 (1998) 627.
[66] (a) A. Deluzet, Ph. D. thesis, University of Nantes, France, 2000;
(b) A. Deluzet, S. Perruchas, H. Bengel, P. Batail, S. Molas, J. Fraxedas, Adv. Funct. Mater. 12 (2002) 123.